

## Tunable Adhesion from Stoichiometry-controlled and Sequence-defined Supramolecular Polymers Emerges Hierarchically from Cyanostar-stabilized Anion-anion Linkages

Wei Zhao, Joshua Tropp, Bo Qiao, Maren Pink, Jason D. Azoulay, and Amar H Flood

*J. Am. Chem. Soc.*, **Just Accepted Manuscript** • Publication Date (Web): 14 Jan 2020

Downloaded from [pubs.acs.org](https://pubs.acs.org) on January 14, 2020

### Just Accepted

“Just Accepted” manuscripts have been peer-reviewed and accepted for publication. They are posted online prior to technical editing, formatting for publication and author proofing. The American Chemical Society provides “Just Accepted” as a service to the research community to expedite the dissemination of scientific material as soon as possible after acceptance. “Just Accepted” manuscripts appear in full in PDF format accompanied by an HTML abstract. “Just Accepted” manuscripts have been fully peer reviewed, but should not be considered the official version of record. They are citable by the Digital Object Identifier (DOI®). “Just Accepted” is an optional service offered to authors. Therefore, the “Just Accepted” Web site may not include all articles that will be published in the journal. After a manuscript is technically edited and formatted, it will be removed from the “Just Accepted” Web site and published as an ASAP article. Note that technical editing may introduce minor changes to the manuscript text and/or graphics which could affect content, and all legal disclaimers and ethical guidelines that apply to the journal pertain. ACS cannot be held responsible for errors or consequences arising from the use of information contained in these “Just Accepted” manuscripts.

# *J. Am. Chem. Soc.*

## **Tunable Adhesion from Stoichiometry-controlled and Sequence-defined Supramolecular Polymers Emerges Hierarchically from Cyanostar-stabilized Anion-anion Linkages**

Wei Zhao,<sup>†</sup> Joshua Tropp,<sup>‡</sup> Bo Qiao,<sup>†,§</sup> Maren Pink,<sup>†</sup> Jason D. Azoulay,<sup>‡</sup> and Amar H. Flood<sup>\*,†</sup>

<sup>†</sup> Department of Chemistry, Indiana University, 800 East Kirkwood Avenue, Bloomington, IN 47405, USA.

<sup>‡</sup> School of Polymer Science and Engineering, The University of Southern Mississippi, 118 College Drive, Hattiesburg, MS 39406, USA.

[aflood@indiana.edu](mailto:aflood@indiana.edu)

**Abstract**

Sequence-controlled supramolecular polymers offer new design paradigms for generating stimuli-responsive macromolecules with enhanced functionalities. The dynamic character of supramolecular links present challenges to sequence definition in extended supramolecular macromolecules, and design principles remain nascent. Here, we demonstrate the first example of using stoichiometry-control to specify the monomer sequence in a linear supramolecular polymer by synthesizing both a homopolymer and an alternating copolymer from the same glycol-substituted cyanostar macrocycle and phenylene-linked diphosphate monomers. A 2:1 stoichiometry between macrocycle and diphosphate produces a supramolecular homopolymer of general formula  $(\mathbf{A})_n$  comprised of repeating units of cyanostar-stabilized phosphate-phosphate dimers. Using a 1:1 stoichiometry, an alternating  $(\mathbf{AB})_n$  structure is produced with half the phosphate dimers now stabilized by the additional counter cations that emerge hierarchically after forming the stronger cyanostar-stabilized phosphate dimers. These new polymer materials and binding motifs are sufficient to bear normal and shear stress to promote significant and tunable adhesive properties. The homopolymer  $(\mathbf{A})_n$ , consisting of cyanostar-stabilized *anti*-electrostatic linkages, shows adhesion strength comparable to commercial superglue formulations based on polycyanoacrylate but is thermally reversible. Unexpectedly, and despite including traditional ionic linkages, the alternating copolymer  $(\mathbf{AB})_n$  shows weaker adhesion strength more similar to commercial white glue based on poly(vinyl acetate). Thus, the adhesion properties can be tuned over a wide range by simply controlling the stoichiometric ratio of monomers. This study offers new insight into supramolecular polymers composed of custom-designed anion and receptor monomers and demonstrates the utility of emerging functional materials based on anion-anion interactions.

## Introduction

Emerging technologies derived from responsive supramolecular polymers<sup>1-2</sup> benefit from the creation of versatile macromolecules with synthetically engineered functionalities.<sup>3-4</sup> Interest in supramolecular polymers<sup>5-7</sup> continues unabated owing to the unique properties conferred by their noncovalent connectivities and dynamic structures,<sup>8-9</sup> as well as their potential for applications in biomedicine,<sup>10-11</sup> optoelectronics,<sup>12-13</sup> and adaptive materials.<sup>14-15</sup> These applications benefit from chemically unique and reconfigurable macromolecular linkages combined with well-defined sequences of monomer units.<sup>6,16</sup> Pioneering efforts to control the sequences of supramolecular polymers have relied on monomers encoded with orthogonal supramolecular linkages, e.g., hydrogen bonding,<sup>17</sup> metal-ligand coordination,<sup>18</sup> and host-guest recognition.<sup>19</sup> These include heterotopic monomers bearing end-groups with orthogonal linkage chemistries,<sup>20-29</sup> and use of two different homotopic monomers with complementary binding partners at either end.<sup>30-33</sup> The orthogonal monomers enable self-sorting to define supramolecular polymer sequences.<sup>28,34</sup> However, use of a single homotopic monomer to achieve sequence control is unknown. This outcome appears to be a contradiction given that the identical end-groups do not offer pre-programmed orthogonality. Here we report the discovery of a single homotopic dianion monomer (Figure 1a) that combines with a macrocycle (Figure 1b) where orthogonal recognition chemistries emerge hierarchically (Figure 1c) to enable control over monomer sequence in homo (Figure 1d) and alternating<sup>35-36</sup> (Figure 1e) supramolecular polymers simply by changing reaction stoichiometry.

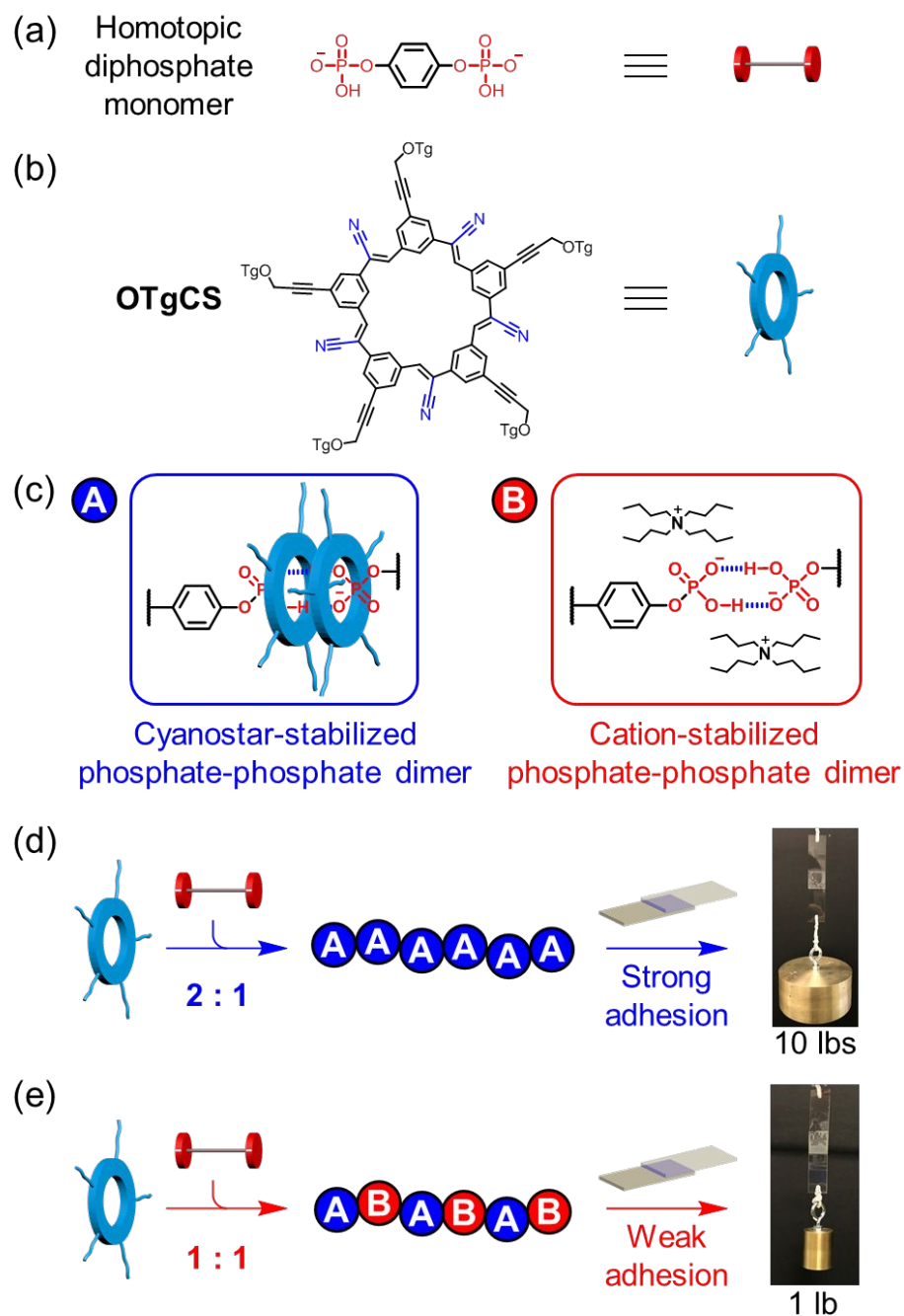


**Figure 1.** Structures of (a) the homotopic diphosphate with a rigid phenylene linker, (b) the new cyanostar macrocycle, **OTgCS**, and linkage chemistries of (c) cyanostar-stabilized phosphate-phosphate dimer (**A**) and cation-stabilized phosphate-phosphate dimer (**B**). Representation of stoichiometry-controlled supramolecular polymers: (d) homopolymer (**A**)<sub>n</sub> shows strong adhesion and (e) the alternating copolymer (**AB**)<sub>n</sub> shows weak adhesion.

1  
2  
3 Previous studies have demonstrated that variation in the reaction stoichiometry of the  
4 monomers can control various features of supramolecular polymers. These include the topology  
5 by toggling between linear and crosslinked states,<sup>37-39</sup> and net chirality.<sup>40-42</sup> Use of the  
6 stoichiometry to control the sequences in linear supramolecular polymers, however, remains  
7 nascent. The role of stoichiometry is well established in small molecule chemistry. Different host-  
8 guest complexes can be made by altering stoichiometry<sup>37-38</sup> but this functionality has yet to be  
9 leveraged for controlling sequences in supramolecular polymers. There are, in general, very few  
10 reported examples of using stoichiometry control. Among them, the closest involves addition of 3  
11 mole% of Eu<sup>2+</sup> to a linear zinc-coordinated supramolecular polymer to drive crosslinking.<sup>39</sup> In  
12 pioneering work from Sessler,<sup>43</sup> stoichiometry was evident when using cationic macrocycles,  
13 called “Texas-sized” boxes, combined with terephthalate monoanions where changing monomer  
14 ratio from 3:2 to 1:1 drove a transition from a small-molecule complex to a supramolecular  
15 polymer. In this case, however, the sequence of the supramolecular polymer was not tunable.  
16 These examples highlight the underdeveloped nature of this approach to control the sequence of  
17 supramolecular polymers. To the best of our knowledge, stoichiometry has not been used to control  
18 the sequence of monomers to form well-defined homo and alternating supramolecular polymers.

19  
20  
21 To construct supramolecular polymers, reliable noncovalent interactions with high affinity  
22 and fidelity are essential.<sup>3</sup> To date, many well-defined recognition chemistries have been  
23 developed and exploited to synthesize supramolecular polymers. The majority of examples are  
24 based upon metal-coordination,<sup>44</sup> hydrogen bonding,<sup>45-46</sup>  $\pi$ - $\pi$  interactions<sup>47-48</sup> and host-guest  
25 interactions.<sup>49-50</sup> Studies involving anion coordination as the driving force for supramolecular  
26 polymerization, however, account for less than 1% of the 10,000+ reports. We<sup>51-52</sup> and  
27 others<sup>21,43,53-59</sup> have recently been working toward filling this gap by exploring the novel

1  
2  
3 noncovalent chemical connectivities promoted by anion receptors and anionic monomers. We  
4 leveraged the high-fidelity dimerization of phosphonate hydroxyanions inside cyanostar  
5 macrocycles as the driving force necessary for the formation of well-defined supramolecular  
6 polymers.<sup>52</sup> The cyanostar-stabilized anion-anion dimer constitutes a 2:2 recognition motif.  
7  
8 Therein, two (2) hydroxyanions dimerize through *anti*-electrostatic hydrogen bonding<sup>60-66</sup> inside a  
9  $\pi$ -stacked pair (2) of cyanostar macrocycles. Although the elementary recognition has been  
10 verified with bisulfate dimers  $(\text{HSO}_4 \cdots \text{HSO}_4)^{2-}$ ,<sup>67-69</sup> dimers of dihydrogen phosphate  
11  $(\text{H}_2\text{PO}_4 \cdots \text{H}_2\text{PO}_4)^{2-}$ ,<sup>70-71</sup> and in polymerization of phosphonate monomers  $(\text{RHPO}_3 \cdots \text{RHPO}_3)^{2-}$ ,<sup>52</sup>  
12 the investigation and development of this anion recognition chemistry into a useful tool for  
13 supramolecular polymer-based materials is far from developed. In our previous study of  
14 supramolecular polymerization driven by phosphonate dimerization,<sup>52</sup> precipitation of a relatively  
15 low molecular-weight product limited subsequent studies to better understand and elucidate the  
16 design principles governing anion-anion driven supramolecular polymerizations.  
17  
18  
19  
20  
21  
22  
23  
24  
25  
26  
27  
28  
29  
30  
31  
32

33  
34 In this present work, we leverage the inherent modularity of anion-anion dimerization to  
35 create new supramolecular connectivities, and present the first example where stoichiometry  
36 generates well-defined supramolecular polymers with controlled sequences. We designed a  
37 cyanostar that is penta-substituted with triethylene glycol chains (**OTgCS**, Figure 1b) to overcome  
38 the solubility issues associated with the parent cyanostar (**tBuCS**).<sup>72</sup> We combined these  
39 macrocycles with a rigid diphosphate monomer bearing two identical phosphate end-groups  
40 connected by a single phenyl ring (Figure 1a). We discovered that the stoichiometric ratio between  
41 building blocks controls the sequence of supramolecular linkages present in the resulting polymers  
42 (Figure 1c). A 2:1 stoichiometry between macrocycle and diphosphate monomer produces a  
43 supramolecular homopolymer, (**A**)<sub>n</sub>, with repeat units of identical 2:2 anion-receptor recognition  
44  
45  
46  
47  
48  
49  
50  
51  
52  
53  
54  
55  
56  
57  
58  
59  
60

1  
2  
3 units. When combined in a 1:1 stoichiometry, however, two types of supramolecular linkages  
4  
5 arranged in an alternating sequence define an alternating copolymer (**AB**)<sub>n</sub>. These links include  
6  
7 the pre-programmed *anti*-electrostatic 2:2 anion-receptor recognition of (**A**), and an unexpected  
8  
9 link, (**B**), based on a phosphate-phosphate dianion dimer stabilized by ion-pairing with the  
10  
11 tetrabutylammonium counter cations (Figure 1c). We demonstrate the use of these materials as a  
12  
13 new class of anion-coordination driven supramolecular polymer adhesives.<sup>73-80</sup> The homopolymer  
14  
15 comprised of cyanostar-stabilized phosphate dimers is sufficiently cohesive to glue hydrophilic  
16  
17 glass slides together to support relatively heavy weights (10 lbs) while the alternating copolymer,  
18  
19 with half the links composed of cation-stabilized anion-anion dimers, shows much weaker  
20  
21 adhesion. We see **OTgCS** macrocycles are also capable of supporting strong adhesion on account  
22  
23 of  $\pi$ -stack mediated self-association of macrocycles. Putative hydrogen bonding from the glass  
24  
25 surface to the **OTgCS** macrocycle's glycol chains operates in concert with the supramolecular  
26  
27 polymerization to promote the adhesion. The adhesion properties correlate to the sequences of the  
28  
29 supramolecular polymers allowing for the development of structure-property relationships for  
30  
31 anion-anion driven supramolecular polymers and design principles for anion-based materials.  
32  
33  
34  
35  
36  
37  
38  
39  
40

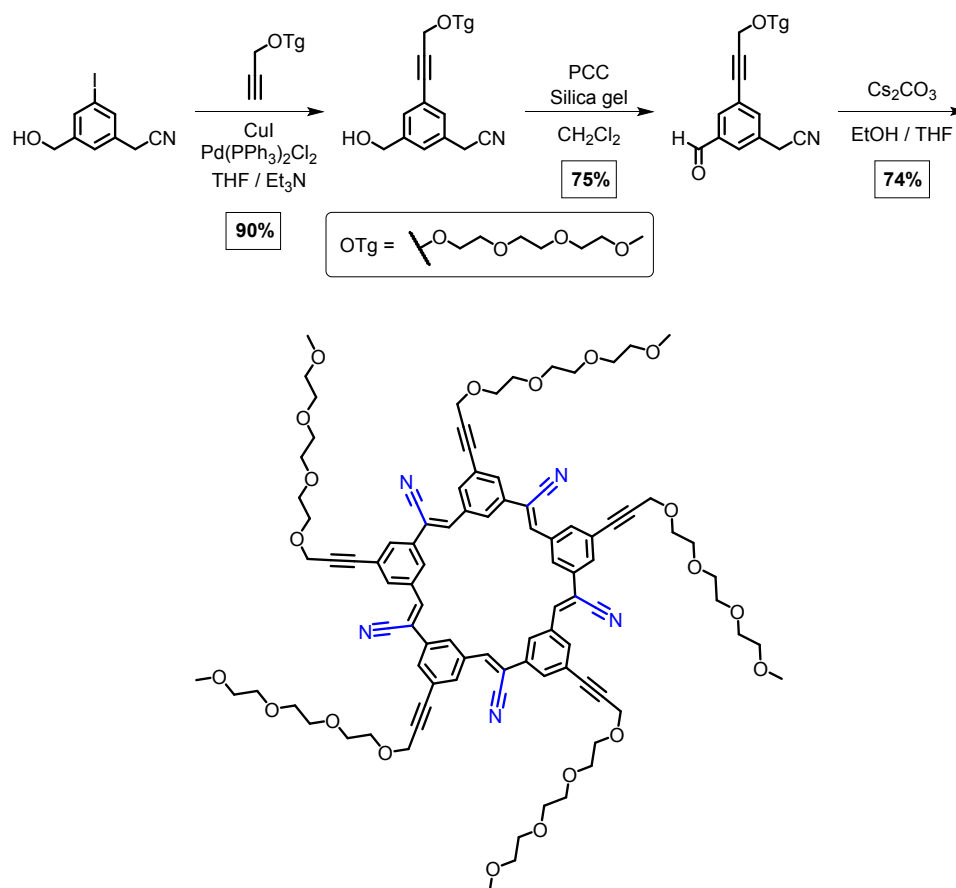
## 41 **Results and Discussion**

### 42 **Molecular Design**

43  
44  
45  
46  
47 The **OTgCS** cyanostar was synthesized with five triethylene glycol chains (Scheme 1) to  
48  
49 enhance solubility for studying polymerization at high concentrations. Ethylene glycol chains are  
50  
51 also commonly incorporated into synthetic adhesives to enable strong hydrogen bonding  
52  
53 interactions with hydrophilic surfaces. The length of the glycol chain was designed to provide  
54  
55  
56  
57  
58  
59  
60

1  
2  
3 sufficient solubility and adhesion properties without adversely impacting purification using  
4 chromatography. The modified **OTgCS** macrocycle was made in good yield following the same  
5 procedure as the parent cyanostar, **tBuCS**.<sup>72</sup> The new cyanostar achieved the desired goals with  
6 enhanced solubility in common organic solvents such as dichloromethane, acetonitrile, and  
7 methanol, and demonstrated a similar anion-binding profile as the parent **tBuCS** macrocycle  
8 towards both  $\text{PF}_6^-$  (Figure S11) and phenyl monophosphate (Figure S12).  
9  
10  
11  
12  
13  
14  
15  
16  
17  
18  
19

20 **Scheme 1.** Synthetic scheme for preparation of penta-substituted cyanostar macrocycle, **OTgCS**.



1  
2  
3 Two types of difunctional monomers were originally designed to help study the  
4 dependence of monomer structure on polymerization. A long flexible monomer, triethylene glycol  
5 bis(phenyl-*p*-phosphate), was used for initial polymerization studies. Its flexibility mimics the  
6 dodecylene diphosphonate we used previously to demonstrate polymerization with **tBuCS**.<sup>52</sup> This  
7 flexible monomer was expected and found to behave similarly, providing confirmation that the  
8 hydroxyanion dimerization could be used as pre-programmed supramolecular links with both  
9 diphosphates as well as the original diphosphonates. To conduct structure-property studies, we  
10 also selected a short and rigid phenylene diphosphate monomer. We initially hypothesized that it  
11 may limit supramolecular polymerization on account of steric interactions and decreased polymer  
12 solubility. We did not anticipate the structural difference between the two monomers would  
13 manifest in the stoichiometric control of supramolecular polymer sequence reported herein.  
14  
15  
16  
17  
18  
19  
20  
21  
22  
23  
24  
25  
26  
27  
28  
29  
30  
31

## 32 **2:2 Model Complex between Phenyl Monophosphate and Cyanostar**

33  
34

35 We used the 2:2 complexation between phenyl monophosphate and the **OTgCS**  
36 macrocycle as a small-molecule model of the linkage chemistry expressed in the supramolecular  
37 polymers. The 2:2 complex forms with high fidelity as seen in a titration monitored by <sup>1</sup>H NMR  
38 spectroscopy (Figure S12). A number of features are similar to the complexation of phenyl  
39 monophosphate with the parent cyanostar **tBuCS**.<sup>70</sup> The uncomplexed **OTgCS** macrocycle shows  
40 similar aromatic peak positions as **tBuCS** (Figure 2a). Upon addition of 1.0 equivalent of phenyl  
41 monophosphate, we see a characteristic signature of the 2:2 linkage (Figure 2b). The far down-  
42 field shifted peak at 14.7 ppm is assigned to the phosphate's OH peak and its position is diagnostic  
43 of the formation of a self-complementary hydrogen bond between the two phosphates and, thus,  
44 confirmation of phosphate dimerization.<sup>67</sup> The anion dimers are formed inside the cavity of  $\pi$ -  
45  
46  
47  
48  
49  
50  
51  
52  
53  
54  
55  
56  
57  
58  
59  
60

stacked macrocycles as established in previous reports.<sup>70</sup> Confirmation of the macrocycle dimers stems from the two  $H_c$  peaks (7.6 ppm, Figure 2b) assigned to diastereomers. Single cyanostars are a racemic mixture of rapidly interconverting  $M$  and  $P$  enantiomers that are known to form into meso ( $MP$ ) and chiral ( $MM$  and  $PP$ ) combinations upon 2:2 complexation.<sup>72,81</sup> Resolution of the two diastereomeric complexes (meso and chiral) indicates exchange between them is slow on the NMR time scale. The formation of the 2:2 complex is also supported by diffusion NMR. The diffusion values obtained from the cyanostar ( $H_c$ ) and the phenylene monophosphate ( $H_f$ ) are identical and generate a volume that is 1.5 times larger than the free macrocycle (Figure 2d).

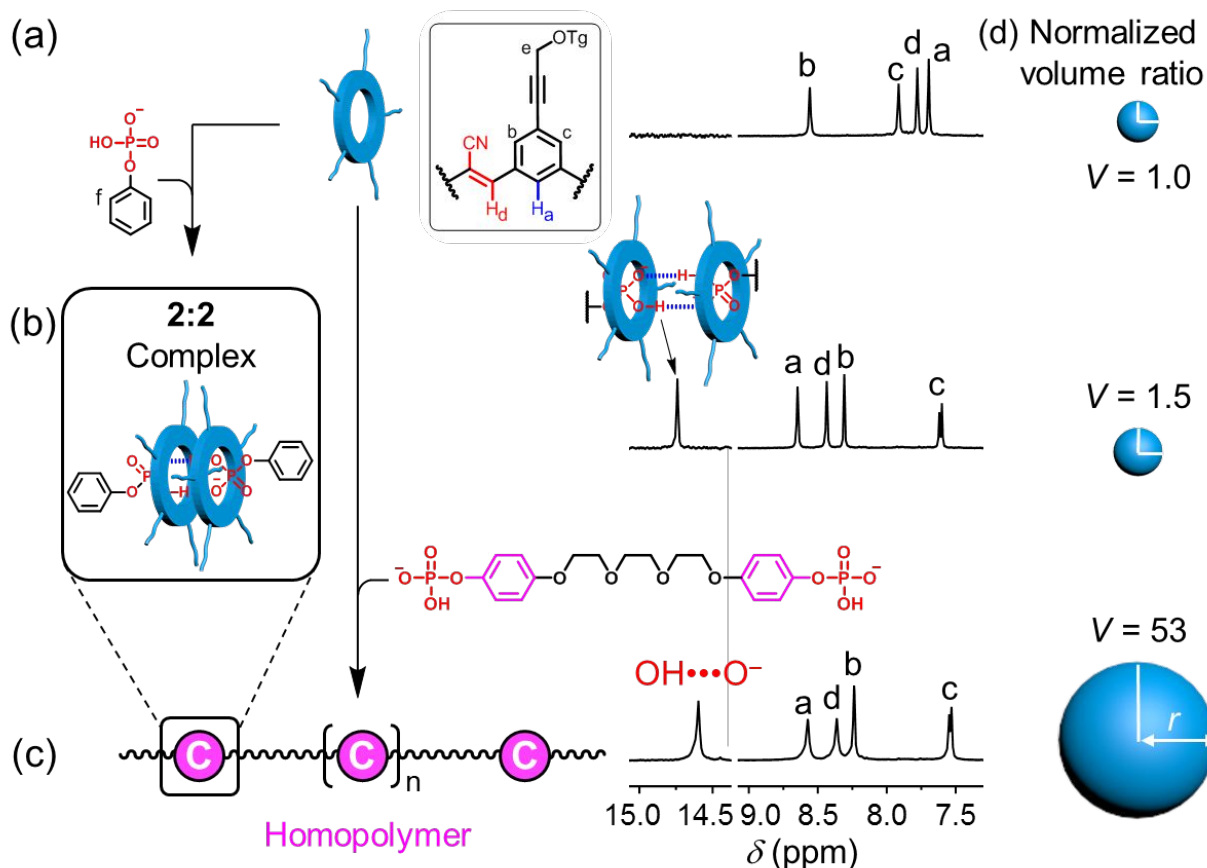


**Figure 2.** Representations and stacked  $^1H$ -NMR spectra of (a) OTgCS, (b) the small-molecule 2:2 complex, and (c) the supramolecular polymer  $(C)_n$ . (d) Normalized size comparisons were

1  
2  
3 determined from diffusion coefficients based on the Stokes-Einstein equation ( $D = \frac{k_B T}{6\pi\eta r}$ ) and the  
4  
5 spherical model ( $V = \frac{4}{3}r^3$ ),  $V$  is proportional to  $\frac{1}{D^3}$ . ([**OTgCS**] = 10 mM, [phenyl monophosphate]  
6  
7 = 10 mM, [triethylene glycol bis(phenyl-*p*-phosphate)] = 5 mM, CD<sub>2</sub>Cl<sub>2</sub>, 298 K, 600 MHz).  
8  
9  
10  
11  
12  
13  
14

### 15 **Supramolecular Homopolymer using the Flexible Diphosphate Monomer**

16  
17  
18 To verify that the diphosphate monomers can be combined with the **OTgCS** macrocycle  
19  
20 to form supramolecular polymers, we used the flexible triethylene glycol bis(phenyl-*p*-phosphate)  
21  
22 to define homopolymers (**C**)<sub>n</sub>. These two components were mixed at a 2:1 ratio to match the  
23  
24 equivalence point for the formation of the 2:2 macrocycle:phosphate linkage chemistry (Figure  
25  
26 2c). Using the 2:2 complex as a model, we see the same diagnostic OH peaks at 14.6 ppm  
27  
28 indicating the formation of the encapsulated phosphate-phosphate dimers (Figure 2c). We also see  
29  
30 characteristic peak shifts (8.1-8.6 ppm) and the diastereomeric splitting in proton H<sub>c</sub> all consistent  
31  
32 with a complexed cyanostar dimer. Together, these observations confirm the formation of the 2:2  
33  
34 linkage chemistry. Indicative of polymerization, the diffusion NMR shows a dramatic 35-fold  
35  
36 increase in size relative to the model complex (Figure 2d). This change is consistent with the 64-  
37  
38 fold difference seen previously with the supramolecular polymer made from **tBuCS** and  
39  
40 dodecylene diphosphonate.<sup>52</sup> These results confirm that supramolecular polymerization can be  
41  
42 achieved using flexible monomers with reliable pre-programmed linkage chemistry composed of  
43  
44 cyanostar-stabilized phosphate dimers.  
45  
46  
47  
48  
49  
50  
51  
52  
53  
54  
55  
56  
57  
58  
59  
60

## Alternating Supramolecular Copolymer in the Solid State using Crystalline Cyanostars

We were surprised to observe a different supramolecular polymer sequence in the solid state when using the rigid phenylene diphosphate monomer in the place of the flexible one. In this case, the more crystalline **tBuCS** cyanostar was used in place of **OTgCS** to determine the crystal structure of the supramolecular polymer. The crystal structure shows two different types of phosphate-phosphate dimers (Figure 3). As expected from all prior studies, we see the 2:2 linkage chemistry highlighted as **(A)**. Therein, the *anti*-electrostatic phosphate-phosphate dimer is encapsulated by two  $\pi$ -stacked macrocycles. The anion dimers are stabilized by a combination of self-complementary hydrogen bonding and the CH hydrogen bonding from the cyanostars.<sup>67,70</sup> The second type of linkage, highlighted as **(B)**, was unanticipated. This new link is also composed of phosphate-phosphate dimers which are not complexed by cyanostars. These dimers engage in one direct phosphate-phosphate hydrogen bond and one methanol-bridged hydrogen bond between the two phosphates. As with all hydroxyanion dimers, theoretical studies<sup>60-64</sup> show that these *anti*-electrostatic hydrogen bonds are insufficient alone to fully stabilize the dimers. Rather, we infer electrostatic stabilization from the close proximity of the four tetrabutylammonium cations (TBA<sup>+</sup>). These cations surround and enshroud the doubly charged phosphate dimers [(RHPO<sub>4</sub>)•••(RHPO<sub>4</sub>)]<sup>2-</sup> (Figure 3). From the six examples<sup>52,67-68,70-71,82</sup> previously studied using cyanostar stabilization, only one<sup>71</sup> shows this type of superstructure when dihydrogen phosphate (H<sub>2</sub>PO<sub>4</sub><sup>-</sup>) was mixed with cyanostar and co-crystallized with an additional equivalent of TBA<sup>+</sup> salt. These types of close anion-cation contacts are more common to salts of hydroxyanion crystallized in the absence of any receptors.<sup>83-84</sup> In those prior cases, such as in the dimer of bisulfate [(HSO<sub>4</sub>)•••(HSO<sub>4</sub>)]<sup>2-</sup> stabilized by tetrabutylammonium,<sup>67</sup> there are an equal number of charged counter cations. In the case here, there are four cations proximal to the two exposed anions.

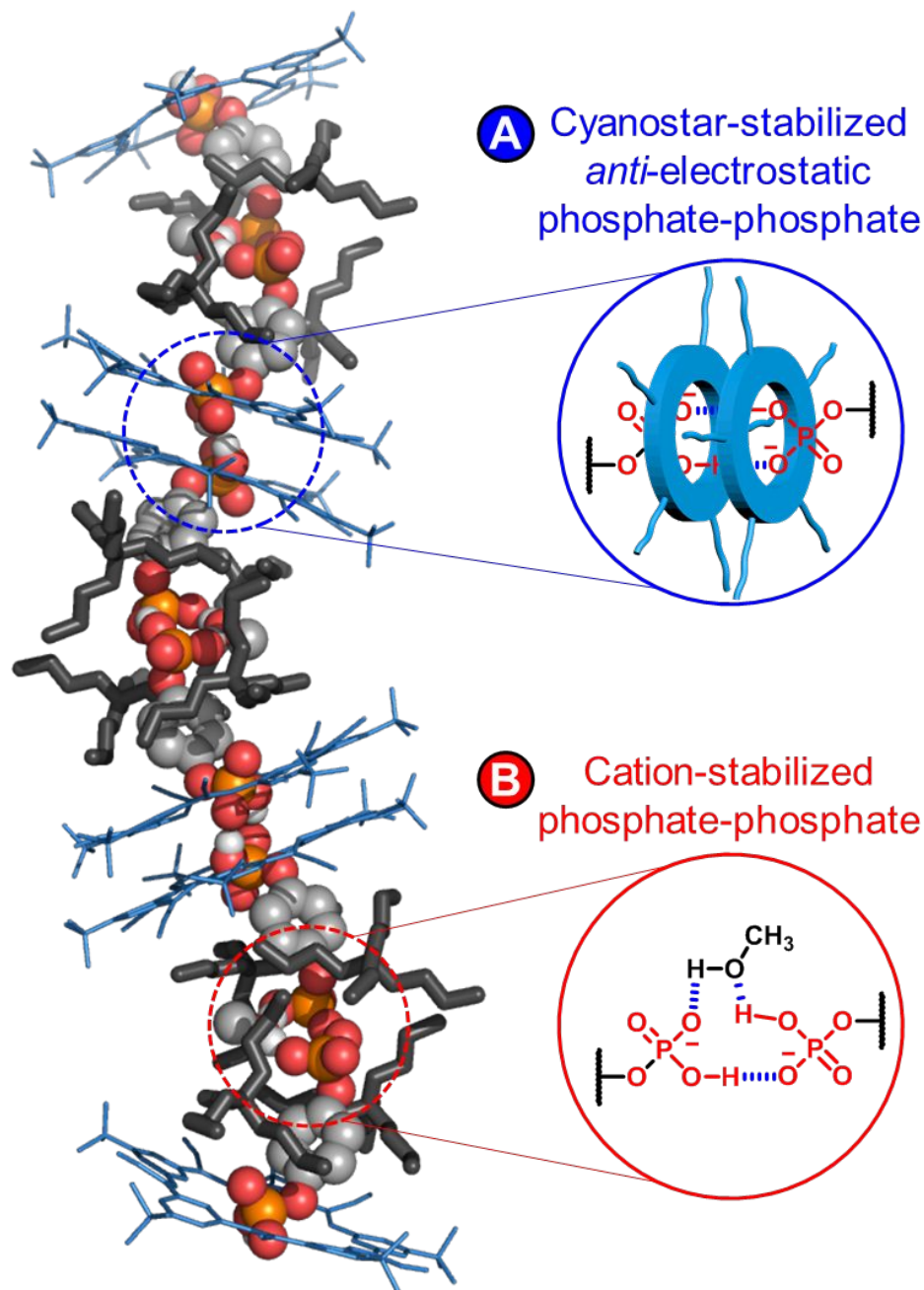


**Figure 3.** Crystal packing structure of the supramolecular copolymer  $(AB)_n$  composed of **tBuCS** macrocycles (blue tube) and phenylene diphosphate (space-filling) as  $TBA^+$  salts (black stick).  $TBA^+$  counter cations encircle the uncomplexed phosphate dimers in **(B)** links. Structures of the phosphate-phosphate dimer encapsulated inside paired macrocycles **(A)** and the methanol-bridged phosphate-phosphate dimer **(B)** are highlighted.

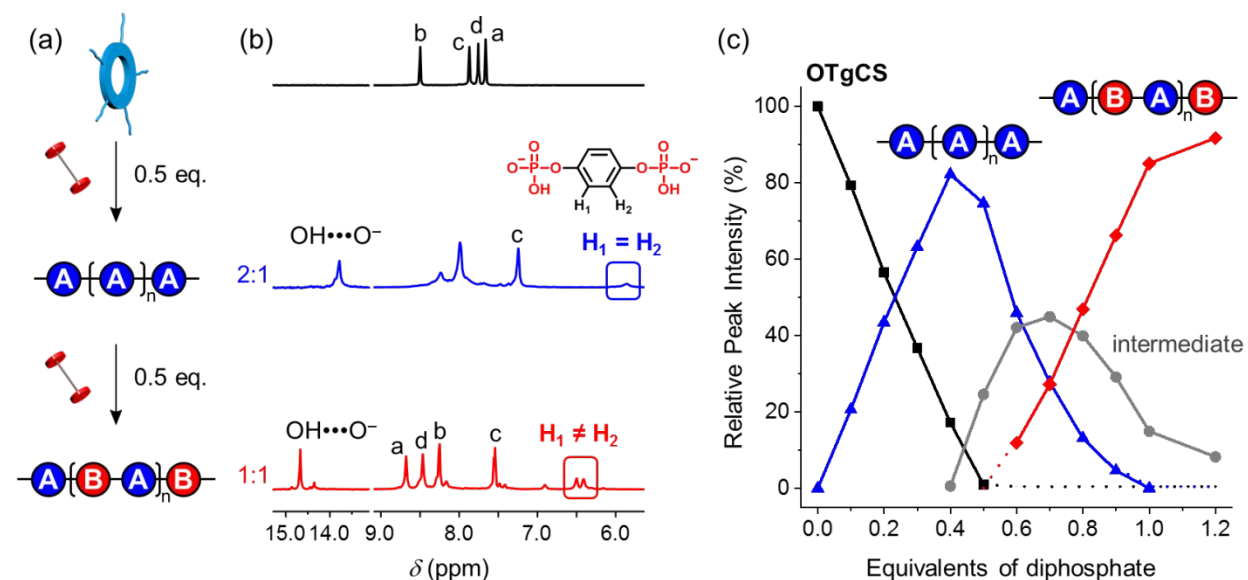
1  
2  
3 The alternating configuration of phosphate dimers, A-B-A-B etc., is believed to come as a  
4 result of the hierarchical assembly in the densely packed solid state. Hierarchical bond formation  
5 dictates that the strongest bonds are formed first followed by the less stable ones. We hypothesized  
6 that the dimers stabilized by the charge-neutral cyanostar macrocycles are stronger than ones  
7 stabilized electrostatically by the counter cations. Consistent with this idea, cyanostar-stabilized  
8 anion-anion dimers are stable in a range of conditions without relying on ion pairing.<sup>68</sup> When the  
9 receptors are not present, anion dimers demand high concentrations to form, offer more ambiguous  
10 signatures and presumably rely on ion pairing for enhanced stabilization.<sup>71</sup> Therefore, formation  
11 of cyanostar-stabilized dimer (**A**) liberates two counter cations for use elsewhere in the assembly.  
12 All together, the uncomplexed phosphate dimers (**B**) have four stabilizing cations. The four cations  
13 emerge from the hierarchical assembly, which is believed to be a key step to forming the  
14 alternating sequence in the copolymer.  
15  
16  
17  
18  
19  
20  
21  
22  
23  
24  
25  
26  
27  
28  
29  
30

31 The distance dependence of electrostatic interactions suggests that the length of the  
32 phenylene linker is also important for copolymer formation. The linker is short enough to help  
33 bring multiple negative charges close to each other to enhance the electrostatic stabilization.<sup>85-86</sup>  
34 Consistent with this idea, use of long dodecylene diphosphonate<sup>52</sup> or the long and flexible  
35 diphosphate monomers fails to produce the alternating copolymer in solution or the solid state. A  
36 competing hypothesis is that the alternating sequence emerges as a result of steric repulsion  
37 between macrocycles. However, the phenylene linker is also long enough to accommodate all the  
38 macrocycles. The goldilocks effect appears to be in play. The phenylene is not too big nor too  
39 small but just right for producing the copolymer. We also attempted to form the homopolymer in  
40 the solid state by increasing the relative amount of **tBuCS** macrocycles during crystallization but  
41 without success. This specific finding suggests that the ionic interactions may be larger than  
42  
43  
44  
45  
46  
47  
48  
49  
50  
51  
52  
53  
54  
55  
56  
57  
58  
59  
60

1  
2  
3 expected. Thus, it was not clear from the crystal structure if the hierarchical assembly of the rigid  
4  
5 phenylene diphosphate into an alternating supramolecular copolymer  $(AB)_n$  is driven by the  
6  
7 cyanostars or the cations.  
8  
9

### 10 11 12 13 Stoichiometry-controlled Supramolecular Copolymers in Solution

14  
15  
16 Inspired by the two types of phosphate-phosphate linkages seen in the crystal structure, we  
17  
18 hypothesized that the alternating copolymer and homopolymer configurations could form in  
19  
20 solution by stoichiometry control (Figure 4a). We expected to produce the supramolecular  
21  
22 homopolymer  $(A)_n$  composed solely of pre-programmed cyanostar-stabilized phosphate dimers by  
23  
24 using a 2:1 stoichiometric ratio between macrocycle and phenylene diphosphate. Adjusting the  
25  
26 stoichiometry to a 1:1 ratio would then be expected to form the alternating supramolecular  
27  
28 copolymer  $(AB)_n$  seen in the solid state.  
29  
30  
31  
32



52  
53  
54 **Figure 4.** (a) Representation for the stoichiometry-controlled supramolecular polymerization. (b)  
55  
56 Stacked  $^1\text{H-NMR}$  spectra of OTgCS, supramolecular homopolymer  $(A)_n$ , and alternating  
57  
58

1  
2  
3 copolymer (**AB**)<sub>n</sub> ([**OTgCS**] = 5 mM, CD<sub>2</sub>Cl<sub>2</sub>, 298 K, 600 MHz). (c) Relative peak intensity  
4 changes of the free macrocycle, the supramolecular homopolymer (**A**)<sub>n</sub>, the alternating  
5 supramolecular copolymer (**AB**)<sub>n</sub> and intermediate species as a function of increasing amount of  
6 phenylene diphosphate.  
7  
8  
9  
10  
11  
12  
13  
14  
15

16 As anticipated, we were able to use stoichiometry to prepare both types of supramolecular  
17 polymers; the (**A**)<sub>n</sub> homopolymer and (**AB**)<sub>n</sub> copolymer. Significantly, the **OTgCS** macrocycle  
18 provided the increased solubility needed to explore stoichiometry control. Elevated concentrations  
19 were not possible using **tBuCS** on account of significant precipitation at the 2:1 ratio beyond 5  
20 mM. The **OTgCS** macrocycle was mixed with 0.5 equivalents of the phenylene diphosphate  
21 monomer to achieve the 2:1 ratio for homopolymerization to form (**A**)<sub>n</sub>. The diagnostic OH peak  
22 at 13.7 ppm indicates the presence of encapsulated phosphate-phosphate dimers in the  
23 supramolecular homopolymer (**A**)<sub>n</sub>. Broad peaks (Figure 4b, middle) in the 7-9 ppm region, which  
24 do not match the sharp peaks (Figure 2c) seen in the homopolymer with the long flexible  
25 diphosphate (**C**)<sub>n</sub>, instead suggest the formation of large aggregates. This interpretation is  
26 consistent with the small diffusion coefficient ( $1.0 \pm 0.2 \times 10^{-10} \text{ m}^2 / \text{s}$ , 5 mM) consistent with 47-  
27 fold larger volume relative to the 2:2 model complex ( $3.7 \pm 0.1 \times 10^{-10} \text{ m}^2 / \text{s}$ , 5 mM).  
28  
29  
30  
31  
32  
33  
34  
35  
36  
37  
38  
39  
40  
41  
42  
43

44 Addition of slightly more diphosphate monomer (e.g., 0.7 equivalents) leads to production  
45 of a more complicated spectrum (Figure S14) attributed to a species of intermediate sequence. We  
46 see decreasing intensity in peaks corresponding to the supramolecular polymer (**A**)<sub>n</sub> around 7.3  
47 ppm (H<sub>c</sub>) and the OH peak at 13.7 ppm. At the same time, a new species is produced represented  
48 by H<sub>c</sub> peaks around 7.4 and 7.5 ppm as well as two OH peaks emerging at 14.3 and 14.6 ppm.  
49 These observations indicate that the encapsulated phosphate-phosphate dimers are in different  
50  
51  
52  
53  
54  
55  
56  
57

1  
2  
3 chemical environments at this intermediate molar ratio. The sequences associated with this  
4 intermediate likely sit between those of the supramolecular homopolymer (**A**)<sub>n</sub> and copolymer  
5  
6  
7  
8 (**AB**)<sub>n</sub>.  
9

10 In order to achieve the correct mole ratio to produce the alternating copolymer (**AB**)<sub>n</sub>, we  
11 added 1.0 equivalent of phenylene diphosphate. Clear cyanostar-based peaks characteristic of the  
12 2:2 linkage chemistry, (**A**), were observed (Figure 4b, bottom). Again, the diffusion coefficient  
13 (1.2 ± 0.1 × 10<sup>-10</sup> m<sup>2</sup> / s) based on peaks in the aromatic region was much smaller than that of the  
14 2:2 complex (3.7 ± 0.1 × 10<sup>-10</sup> m<sup>2</sup> / s), corresponding to a species that is 27-fold larger. The OH  
15 peak at 14.6 ppm confirms the phosphate-phosphate dimers are encapsulated inside the cyanostar  
16 dimers. The hydrogen-bonded OH protons of the uncomplexed phosphate-phosphate dimers  
17 cannot be identified from the <sup>1</sup>H NMR spectra. This finding is consistent with previous studies<sup>71</sup>  
18 involving complexation of dihydrogen phosphate H<sub>2</sub>PO<sub>4</sub><sup>-</sup> dimers and trimers with **tBuCS**.  
19 Diagnostic of the structure of the alternating copolymer, we see the phenylene monomer's  
20 symmetry is broken and gives rise to two peaks of equal intensity at 6.5 and 6.4 ppm. (Figure S18).  
21 We also see two peaks in the <sup>31</sup>P NMR spectra (Figure S20). Consistently, we only see one  
22 resonance from the homopolymer (**A**)<sub>n</sub>. The two different chemical environments coincide with  
23 the crystal packing structure of the alternating copolymer (**AB**)<sub>n</sub> (Figure 3).  
24  
25  
26  
27  
28  
29  
30  
31  
32  
33  
34  
35  
36  
37  
38  
39  
40  
41  
42

43 Structural evidence for the alternating copolymer is provided from the <sup>1</sup>H-<sup>1</sup>H NOESY  
44 correlations. First, we observe a crosspeak from the phenylene ring of the diphosphate monomer  
45 (Figure 5, H<sub>1</sub>, H<sub>2</sub>) to the protons (H<sub>α</sub>) on the TBA<sup>+</sup> counter cations indicative of the ion-pairing  
46 interactions expected for the unencapsulated phosphate-phosphate dimers. These ion-pair  
47 interactions must be reasonably long lived to generate NOE crosspeaks. This cross peak is not seen  
48 in the homopolymer (**A**)<sub>n</sub>. Correlation peaks in the <sup>1</sup>H-<sup>1</sup>H NOESY plot (Figure S30) between the  
49  
50  
51  
52  
53  
54  
55  
56  
57  
58  
59  
60

1  
2  
3 protons inside macrocycles cavity ( $H_a$ ,  $H_d$ ) and on the phenylene diphosphate ( $OH$ ,  $H_1$ ,  $H_2$ ) also  
4 support formation of the cyanostar-stabilized phosphate dimer. All these results are consistent with  
5 support formation of the cyanostar-stabilized phosphate dimer. All these results are consistent with  
6 support formation of the cyanostar-stabilized phosphate dimer. All these results are consistent with  
7 the two different forms of the phosphate-phosphate dimers in the alternating copolymer. If instead  
8 a random or statistical sequence was present, e.g., AABABBBBA, we would expect a larger number  
9 of  $^1H$  NMR peaks associated with the greater variety of chemical environments. As we only see  
10 two major peaks for the phenyl ring of the phenylene diphosphate in a 1:1 ratio, an alternating  
11 two major peaks for the phenyl ring of the phenylene diphosphate in a 1:1 ratio, an alternating  
12 two major peaks for the phenyl ring of the phenylene diphosphate in a 1:1 ratio, an alternating  
13 two major peaks for the phenyl ring of the phenylene diphosphate in a 1:1 ratio, an alternating  
14 two major peaks for the phenyl ring of the phenylene diphosphate in a 1:1 ratio, an alternating  
15 two major peaks for the phenyl ring of the phenylene diphosphate in a 1:1 ratio, an alternating  
16 two major peaks for the phenyl ring of the phenylene diphosphate in a 1:1 ratio, an alternating  
17 two major peaks for the phenyl ring of the phenylene diphosphate in a 1:1 ratio, an alternating  
18 two major peaks for the phenyl ring of the phenylene diphosphate in a 1:1 ratio, an alternating  
19 two major peaks for the phenyl ring of the phenylene diphosphate in a 1:1 ratio, an alternating  
20 two major peaks for the phenyl ring of the phenylene diphosphate in a 1:1 ratio, an alternating  
21 two major peaks for the phenyl ring of the phenylene diphosphate in a 1:1 ratio, an alternating  
22 two major peaks for the phenyl ring of the phenylene diphosphate in a 1:1 ratio, an alternating  
23 two major peaks for the phenyl ring of the phenylene diphosphate in a 1:1 ratio, an alternating  
24 two major peaks for the phenyl ring of the phenylene diphosphate in a 1:1 ratio, an alternating  
25 two major peaks for the phenyl ring of the phenylene diphosphate in a 1:1 ratio, an alternating  
26 two major peaks for the phenyl ring of the phenylene diphosphate in a 1:1 ratio, an alternating  
27 two major peaks for the phenyl ring of the phenylene diphosphate in a 1:1 ratio, an alternating  
28 two major peaks for the phenyl ring of the phenylene diphosphate in a 1:1 ratio, an alternating  
29 two major peaks for the phenyl ring of the phenylene diphosphate in a 1:1 ratio, an alternating  
30 two major peaks for the phenyl ring of the phenylene diphosphate in a 1:1 ratio, an alternating  
31 two major peaks for the phenyl ring of the phenylene diphosphate in a 1:1 ratio, an alternating  
32 two major peaks for the phenyl ring of the phenylene diphosphate in a 1:1 ratio, an alternating  
33 two major peaks for the phenyl ring of the phenylene diphosphate in a 1:1 ratio, an alternating  
34 two major peaks for the phenyl ring of the phenylene diphosphate in a 1:1 ratio, an alternating  
35 two major peaks for the phenyl ring of the phenylene diphosphate in a 1:1 ratio, an alternating  
36 two major peaks for the phenyl ring of the phenylene diphosphate in a 1:1 ratio, an alternating  
37 two major peaks for the phenyl ring of the phenylene diphosphate in a 1:1 ratio, an alternating  
38 two major peaks for the phenyl ring of the phenylene diphosphate in a 1:1 ratio, an alternating  
39 two major peaks for the phenyl ring of the phenylene diphosphate in a 1:1 ratio, an alternating  
40 two major peaks for the phenyl ring of the phenylene diphosphate in a 1:1 ratio, an alternating  
41 two major peaks for the phenyl ring of the phenylene diphosphate in a 1:1 ratio, an alternating  
42 two major peaks for the phenyl ring of the phenylene diphosphate in a 1:1 ratio, an alternating  
43 two major peaks for the phenyl ring of the phenylene diphosphate in a 1:1 ratio, an alternating  
44 two major peaks for the phenyl ring of the phenylene diphosphate in a 1:1 ratio, an alternating  
45 two major peaks for the phenyl ring of the phenylene diphosphate in a 1:1 ratio, an alternating  
46 two major peaks for the phenyl ring of the phenylene diphosphate in a 1:1 ratio, an alternating  
47 two major peaks for the phenyl ring of the phenylene diphosphate in a 1:1 ratio, an alternating  
48 two major peaks for the phenyl ring of the phenylene diphosphate in a 1:1 ratio, an alternating  
49 two major peaks for the phenyl ring of the phenylene diphosphate in a 1:1 ratio, an alternating  
50 two major peaks for the phenyl ring of the phenylene diphosphate in a 1:1 ratio, an alternating  
51 two major peaks for the phenyl ring of the phenylene diphosphate in a 1:1 ratio, an alternating  
52 two major peaks for the phenyl ring of the phenylene diphosphate in a 1:1 ratio, an alternating  
53 two major peaks for the phenyl ring of the phenylene diphosphate in a 1:1 ratio, an alternating  
54 two major peaks for the phenyl ring of the phenylene diphosphate in a 1:1 ratio, an alternating  
55 two major peaks for the phenyl ring of the phenylene diphosphate in a 1:1 ratio, an alternating  
56 two major peaks for the phenyl ring of the phenylene diphosphate in a 1:1 ratio, an alternating  
57 two major peaks for the phenyl ring of the phenylene diphosphate in a 1:1 ratio, an alternating  
58 two major peaks for the phenyl ring of the phenylene diphosphate in a 1:1 ratio, an alternating  
59 two major peaks for the phenyl ring of the phenylene diphosphate in a 1:1 ratio, an alternating  
60 two major peaks for the phenyl ring of the phenylene diphosphate in a 1:1 ratio, an alternating

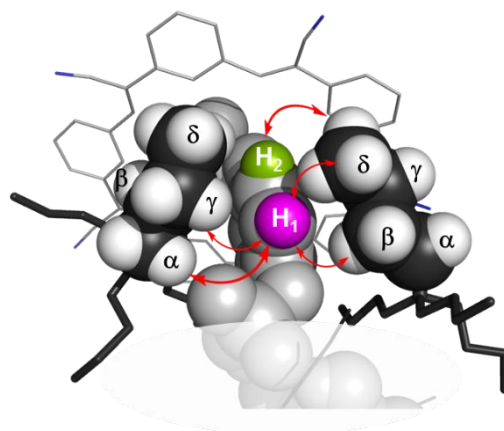
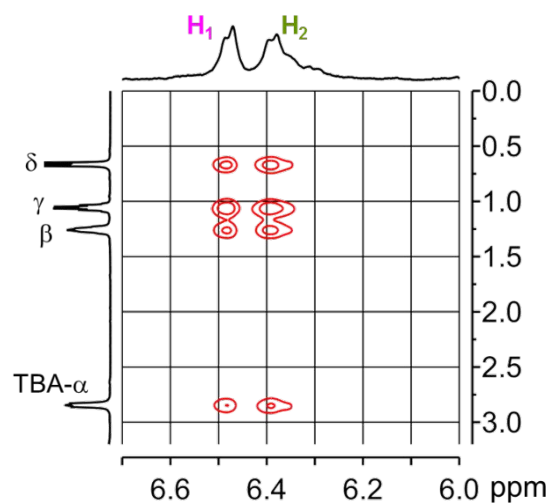


**Figure 5.** Partial  $^1H$ - $^1H$  NOESY spectra of the alternating copolymer shows correlations between TBA<sup>+</sup> cation and the phenylene diphosphate monomers. ( $[OTgCS] = 5$  mM,  $CD_2Cl_2$ , 298 K, 500 MHz).

1  
2  
3 To the best of our knowledge, this is the first time that stoichiometry has been shown to  
4 control the sequence of supramolecular polymers. We can plot the species variation as a function  
5 of stoichiometry using the signatures assigned to the homopolymer ( $\mathbf{A}$ )<sub>n</sub> and alternating copolymer  
6 ( $\mathbf{AB}$ )<sub>n</sub> (Figure 4c). For this speciation plot, we used a combination of the OH peaks and the  
7 aromatic peaks in the 7.0-7.6 ppm region to determine relative peak intensities (Figure S14). We  
8 also include the intermediate species by using the OH peak at 14.3. In the speciation curve (Figure  
9 4c), we see the supramolecular homopolymer ( $\mathbf{A}$ )<sub>n</sub> dominates at 2:1 stoichiometry (0.5 equivalents)  
10 and the alternating copolymer ( $\mathbf{AB}$ )<sub>n</sub> dominates at the 1:1 stoichiometry (1.0 equivalent).  
11  
12  
13  
14  
15  
16  
17  
18  
19  
20  
21

22 In order to understand the concentration-dependence for the stoichiometry-controlled  
23 supramolecular polymerization, we repeated the titrations at lower ( $[\mathbf{OTgCS}] = 0.5 \text{ mM}$ ) and  
24 higher ( $[\mathbf{OTgCS}] = 50 \text{ mM}$ ) concentrations (Figure S16 and S17). We see the distribution of  
25 species largely remains the same with increasing concentration.  
26  
27  
28  
29  
30  
31  
32  
33  
34

### 35 **Concentration-driven Supramolecular Polymerization**

36  
37 Increasing the concentration of monomers is known to drive supramolecular  
38 polymerization. Consistently, diffusion NMR studies show the size of the both ( $\mathbf{A}$ )<sub>n</sub> and ( $\mathbf{AB}$ )<sub>n</sub>  
39 polymers show a 21-fold and 87-fold volume change from 1 mM to 50 mM, respectively (Figure  
40 6a). For the phenylene diphosphate alone, however, diffusion coefficients show a small decrease  
41 indicating a 2.6-fold volume change consistent with a previous study for the dodecylene  
42 diphosphonate.<sup>52</sup> These results suggest that cyanostar-stabilized anion-anion dimers are  
43 responsible for the driving force of supramolecular polymerization. We also see the diffusion  
44 coefficients for the ( $\mathbf{AB}$ )<sub>n</sub> copolymer becomes larger than ( $\mathbf{A}$ )<sub>n</sub> at concentrations above 50 mM.  
45  
46  
47  
48  
49  
50  
51  
52  
53  
54  
55  
56 This result is consistent with increased ion pairing helping to stabilize the uncomplexed phosphate-  
57  
58  
59  
60

phosphate dimers at higher concentrations. We also see from these results that the diffusion coefficient of the **OTgCS** macrocycle decreases over this concentration range. This behavior is indicative of self-association facilitated by  $\pi$ - $\pi$  interactions between the faces of **OTgCS** macrocycles. Variable concentration studies followed by NMR spectroscopy show that this macrocycle aggregates more than the parent cyanostar consistent with the role of glycol chains in stabilizing self-associated stacks of shape persistent macrocycles (Figure S9).<sup>87-88</sup>

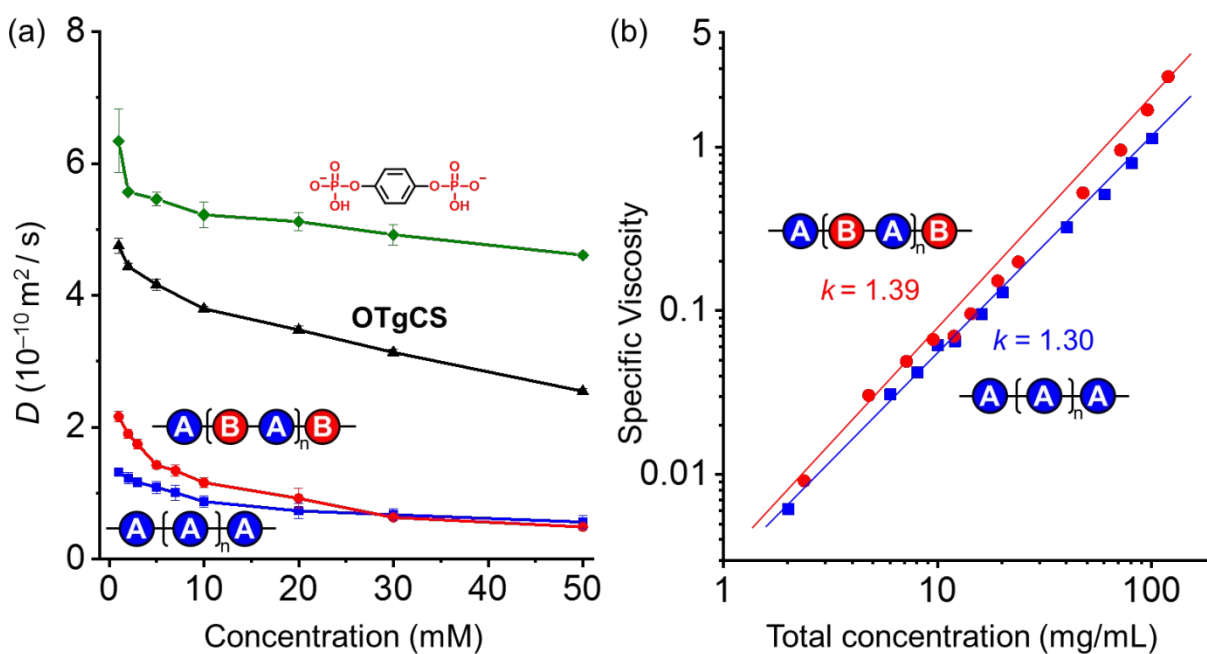


**Figure 6.** (a) Changes of diffusion coefficients of the phenylene diphosphate, **OTgCS**, and **OTgCS** with 0.5 equiv. and 1.0 equiv. of phenylene diphosphate with increasing concentration. (b) Specific viscosity of the homopolymer and the alternating copolymer versus concentration change in mg / mL (dichloromethane, 298 K, 600 MHz).

1  
2  
3 To further verify the concentration-driven polymerization, we conducted specific viscosity  
4 measurements (Figure 6b). The double-logarithmic plots of specific viscosity versus concentration  
5 for supramolecular polymers  $(\mathbf{A})_n$  and  $(\mathbf{AB})_n$  display slopes of 1.30 and 1.39, respectively. We see  
6 the alternating copolymer shows a slightly larger slope than the homopolymer suggesting the  
7 alternating copolymer is more likely to be physically entangled.<sup>89</sup> A turning point in these plots  
8 are sometimes observed and then assigned to the critical polymerization concentration (CPC).<sup>90</sup>  
9 The absence of such a point over the concentration range examined here suggests that  $(\mathbf{A})_n$  and  
10  $(\mathbf{AB})_n$  are already above the CPC for both polymers. This type of behavior has been seen  
11 previously in supramolecular polymers that were promoted by rigid monomers.<sup>17,45</sup>  
12  
13  
14  
15  
16  
17  
18  
19  
20  
21  
22  
23  
24  
25  
26  
27

### 28 **Stoichiometry-controlled Adhesion Properties of the Supramolecular Polymers**

29  
30  
31 Structure-property relationships can be established by correlating the different  
32 supramolecular polymer sequences,  $(\mathbf{A})_n$  and  $(\mathbf{AB})_n$  to their adhesive properties. In contrast to the  
33 supramolecular polymer based on the parent macrocycle **tBuCS**, we did not observe precipitation  
34 when using **OTgCS** thereby allowing for further study of its bulk properties. The supramolecular  
35 polymers derived from **OTgCS** are sticky and viscous at high concentration. Inspired by this  
36 observation and other supramolecular polymer adhesives,<sup>73</sup> we hypothesized that the **OTgCS**-  
37 based supramolecular polymers could be used as adhesive materials. Specifically, for binding  
38 hydrophilic surfaces together (Figure 7a), such as glass, on account of OH•••O hydrogen bonding  
39 from surface hydroxyls (SiOH) to the ether oxygens in the triethylene glycol chains of the **OTgCS**  
40 macrocycle (Figure 7b).<sup>74,78</sup>  
41  
42  
43  
44  
45  
46  
47  
48  
49  
50  
51  
52  
53  
54  
55  
56  
57  
58  
59  
60

1  
2  
3 Each supramolecular polymer was used to coat glass slides with a  $2.5 \times 2.5 \text{ cm}^2$  overlap  
4 area and the resulting slides were used to support weights for initial adhesion testing (Figure 7c).  
5  
6 We observed that the **OTgCS** macrocycle alone is capable of supporting a 10-lb weight (Figure  
7  
8 7c, left). This behavior is attributed to the self-aggregation of **OTgCS** macrocycles seen in the  
9  
10 variable concentration studies monitored by diffusion NMR (Figure 6a) and  $^1\text{H}$  NMR spectroscopy  
11  
12 (Figure S9). Assuming the  $\pi$ -stacking between **OTgCS** macrocycles dominate the self-assembly,  
13  
14 the triethylene glycol chains are free to interact with the hydrophilic surface through hydrogen  
15  
16 bonding. Pull-off (Figure 8a) and lap-shear (Figure S35) adhesion tests were performed to quantify  
17  
18 the adhesion strength of **OTgCS** (Table 1). The **OTgCS** macrocycle shows strong pull-off tensile  
19  
20 strength of  $3.6 \pm 0.4 \text{ MPa}$  and shear strength of  $1.6 \pm 0.6 \text{ MPa}$ . For comparison, the **tBuCS**  
21  
22 macrocycle did not display any adhesive properties, which supports the significant role of the  
23  
24 triethylene glycol chains in adhesion.  
25  
26  
27  
28  
29  
30  
31  
32  
33  
34  
35  
36  
37  
38  
39  
40  
41  
42  
43  
44  
45  
46  
47  
48  
49  
50  
51  
52  
53  
54  
55  
56  
57  
58  
59  
60

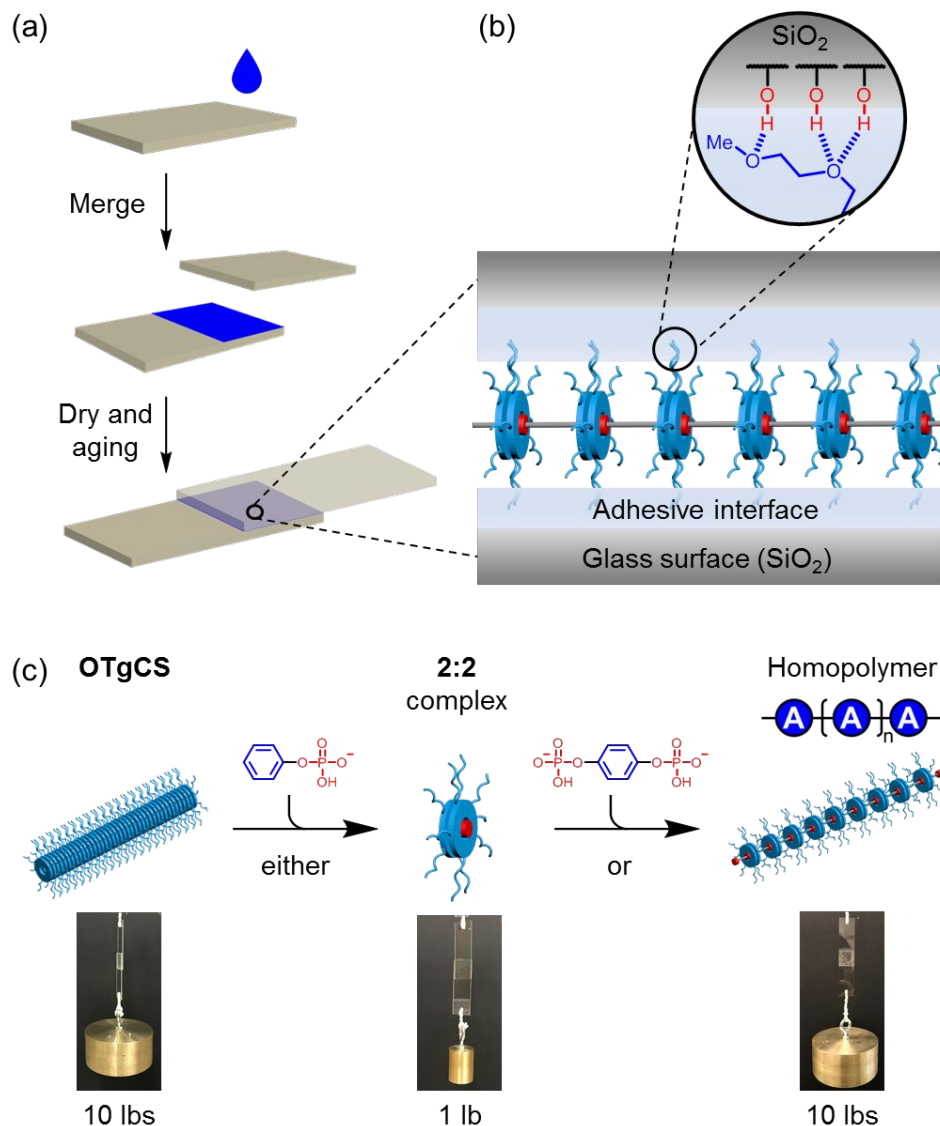


**Figure 7.** (a) Schematic procedure of preparing adhesive samples using glass slides. (b) Representation of the hydrogen bonding interaction between hydrophilic glass surface and the triethylene glycol chains from **OTgCS** macrocycles on the polymer. (c) Photographs showing adhesion behavior of **OTgCS**, the 2:2 complex of **OTgCS** and phenyl monoposphate, and the supramolecular homopolymer of  $(\text{A})_n$  using the phenylene diphosphate, respectively. Adhesive sample loading is 10 mg, and loading area is  $2.5 \times 2.5 \text{ cm}^2$ .

For the small-molecule 2:2 complex between the **OTgCS** macrocycle and phenyl monophosphate, we observed very weak adhesion that only supported a 1-lb weight (Figure 7c, middle), with a pull-off adhesion strength of  $0.5 \pm 0.2$  MPa, and shear strength of  $0.2 \pm 0.1$  MPa (Table 1). The weaker adhesion strength is consistent with loss of macrocycle self-association upon complexation. This change from associated state to a complex has been seen with a related tricarbozole macrocycle that displays a high degree of self-association.<sup>69</sup> Thus, while the hydrogen bonding between the surface and the glycol chains is important for strong adhesion when using the **OTgCS** macrocycles, addition of the custom-designed organophosphate anions to drive formation of 2:2 complexes is insufficient to create an adhesive material.

**Table 1.** Quantitative adhesion strength of supramolecular polymers, control monomers, 2:2 complex, commercial glues and other supramolecular polymer adhesives.<sup>a</sup>

Sample	Pull-off strength (MPa)	Lap-shear strength (MPa)
<b>OTgCS</b>	$3.6 \pm 0.4$	$1.6 \pm 0.6$
<b>2:2</b> complex	$0.5 \pm 0.2$	$0.2 \pm 0.1$
( <b>A</b> ) <sub>n</sub>	$4.2 \pm 0.4$	$2.0 \pm 0.5$
( <b>AB</b> ) <sub>n</sub>	$0.9 \pm 0.2$	$0.4 \pm 0.2$
( <b>C</b> ) <sub>n</sub>	$2.4 \pm 0.3$	$1.1 \pm 0.2$
Superglue	5 ~ 9	—
White glue	0.4	—
Hydrogen bonding driven SPS <sup>b</sup>	4.2	—
Metal-coordination SPS <sup>c</sup>	—	2.5

1  
2  
3 <sup>a</sup> Sample loading of tested materials is about 10 mg, loading area is  $2.5 \times 2.5 \text{ cm}^2$ . <sup>b</sup> Hydrogen  
4 bonding driven supramolecular polymer using triply benzo-21-crown-7-substituted 1,3,5-  
5 benzenetricarboxamides.<sup>74</sup> <sup>c</sup> Metal-coordination driven supramolecular polymer based on iron  
6 coordinated poly(thioctic acid diisopropenylbenzene).<sup>78</sup>  
7  
8  
9  
10  
11  
12  
13  
14  
15

16 Strong adhesion is expected from the supramolecular polymers where the 2:2 linkages are  
17 now covalently linked together. Consistently, we see the supramolecular homopolymer (**A**)<sub>n</sub>  
18 supports a 10-lb weight (Figure 7c, right), with a pull-off strength of  $4.2 \pm 0.4 \text{ MPa}$  (Figure 8b).  
19 This adhesion strength is comparable to supramolecular adhesive made using  
20 benzenetricarboxamide triply substituted with benzo-21-crown-7 ( $4.2 \text{ MPa}$ ),<sup>74</sup> and which relies on  
21 hydrogen bonding linkages. By doing a single lap-shear test, we see the supramolecular  
22 homopolymer shows a shear strength ( $2.0 \pm 0.5 \text{ MPa}$ ), which is comparable to a metal coordination  
23 driven supramolecular copolymer based on poly(thioctic acid diisopropenylbenzene) ( $2.5 \text{ MPa}$ ).<sup>78</sup>  
24 It is clear from this performance that anion-driven supramolecular polymers display adhesion  
25 properties that match supramolecular polymers supported by more traditional linkage chemistries.  
26 Nevertheless, it is counterintuitive that the strong adhesion arises from linkage chemistry involving  
27 two like charges. These linkages are expected to repel each other and inhibit, instead of enhance,  
28 adhesion. The fact that this expectation is not fulfilled is remarkable and underscores the role of  
29 cyanostar recognition in helping reshape the terms of conventional wisdom.  
30  
31  
32  
33  
34  
35  
36  
37  
38  
39  
40  
41  
42  
43  
44  
45  
46  
47  
48

49 In the case of the alternating copolymer (**AB**)<sub>n</sub>, exactly half of the cyanostar-stabilized  
50 linkages are replaced by cation-stabilized linkages such that every other phosphate-phosphate  
51 dianion (2<sup>-</sup>) is stabilized by four proximal cations (4<sup>+</sup>). This system falls squarely in the realms  
52 of our conventional wisdom where the attraction between opposite charges is expected to  
53  
54  
55  
56  
57  
58  
59  
60

contribute to significant stabilization in the solid state. Furthermore, solids typically support closer contacts and lower dielectric constants than solutions. From Coulomb's law, therefore, this ionic bonding is expected to be substantial. It is not clear *a priori*, therefore, if the bulk samples of the homopolymer  $(A)_n$  or the copolymer  $(AB)_n$  would have stronger adhesion.

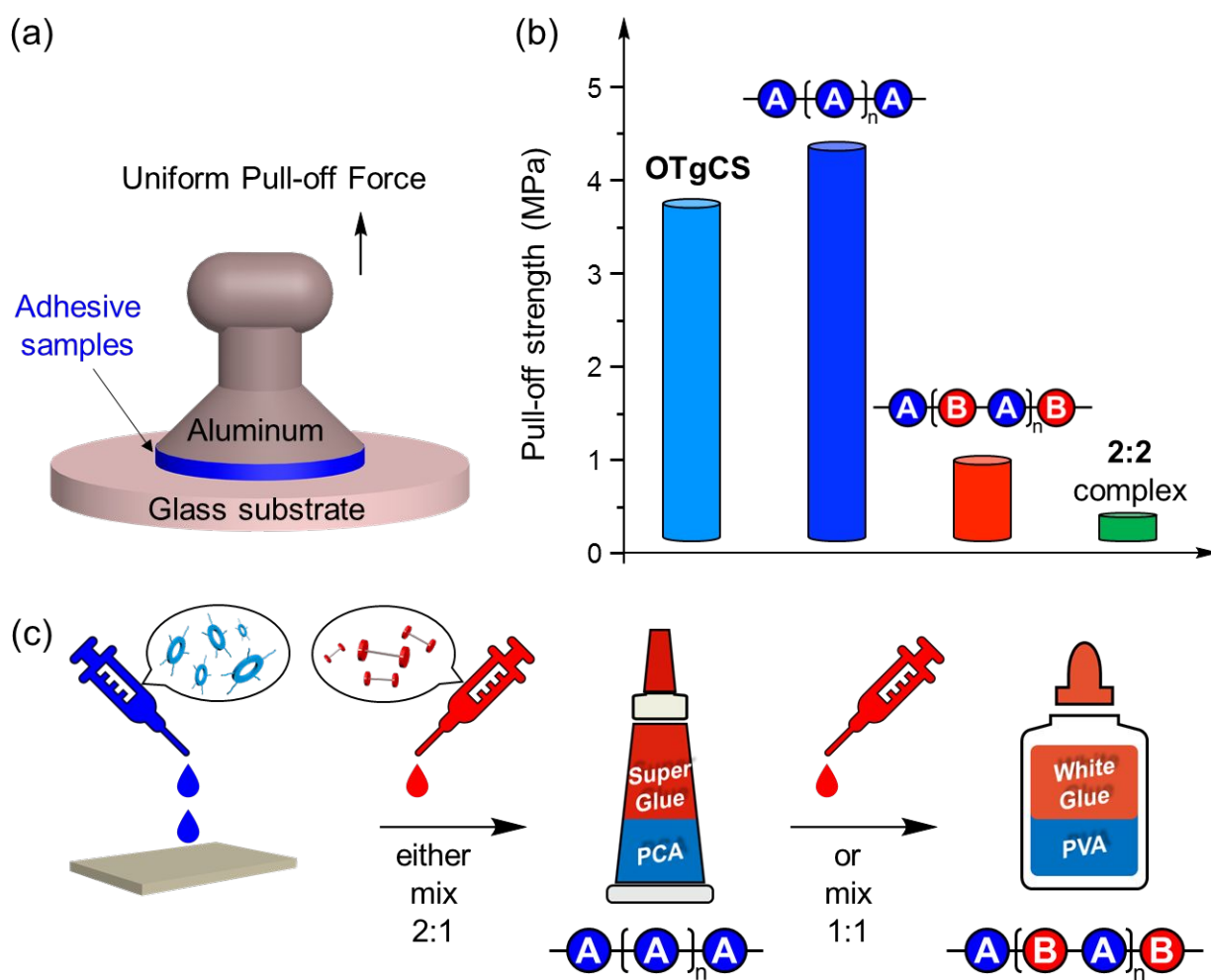


**Figure 8.** (a) Representation of the pull-off strength test for adhesive samples. (b) Pull-off strength of OTgCS, the 2:2 complex between OTgCS and phenyl monophosphate, the supramolecular homopolymer  $(A)_n$ , and the copolymer  $(AB)_n$  using the phenylene diphosphate. (c) Representation

1  
2  
3 of tunable supramolecular polymer adhesives made from a two-pot mix into either the superglue  
4 grade homopolymer or white glue grade copolymer.  
5  
6  
7  
8  
9

10  
11 A much weaker adhesion strength was observed for the alternating supramolecular  
12 copolymer (**AB**)<sub>n</sub> than the homopolymer (**A**)<sub>n</sub>. A pull-off strength of  $0.9 \pm 0.2$  MPa and a shear  
13 strength is  $0.4 \pm 0.2$  MPa were observed (Figure 8b). The copolymer is only about 20% the  
14 adhesion strength of the homopolymer. This observation strongly suggests that the linkage defined  
15 by cyanostar-stabilized *anti*-electrostatic phosphate dimers are stronger than the cation-stabilized  
16 phosphate dimers.  
17  
18  
19  
20  
21  
22  
23  
24

25 To provide some support for the roles of cyanostar-stabilized and cation-stabilized anion-  
26 anion linkages, we conducted a series of control studies. To enhance the electrostatic driving force,  
27 we added extra TBA<sup>+</sup> salts and consistently saw increases in the adhesion strength (Figure S32) of  
28 the alternating copolymer. To test for the role of the cyanostar in adhesion, we evaluated a neat  
29 film of the phenylene diphosphate monomer alone. No adhesion was observed, which is attributed  
30 to the absence of surface-active glycols. To emulate the surface interaction, we mixed the rigid  
31 monomer with 1 equivalent of polyethylene glycol of a molecular weight ( $M_w = 2000$  g mol<sup>-1</sup>)  
32 matching two cyanostars used in homopolymer (**A**)<sub>n</sub>. No adhesion was observed in this case either  
33 (Figure S33). These results support the finding that the anion-anion linkages also benefit  
34 substantially from cyanostar stabilization. We evaluated the adhesion strength (Table 1) of the  
35 supramolecular polymer (**C**)<sub>n</sub> composed of the flexible triethylene glycol bis(phenyl-*p*-phosphate)  
36 and found it is about half that of (**A**)<sub>n</sub> despite having the same amount of cyanostar in each case.  
37 This result suggests that the compact character of the supramolecular polymer chain in (**A**)<sub>n</sub>  
38 provides better support for adhesion.  
39  
40  
41  
42  
43  
44  
45  
46  
47  
48  
49  
50  
51  
52  
53  
54  
55  
56  
57

## Reversible and Tunable Adhesion

The adhesion properties of the supramolecular homopolymer (**A**)<sub>n</sub> are thermally reversible. A 10-lb weight was released by external heating (~50-60°C) of the bonded glass slides for ~30 s (Figure S34). We observe that both faces of the debonded glass slides retain some of the supramolecular adhesive material indicating that the debonding occurred within the adhesive material. This heat-induced debonding can be attributed to either the loss of physical entanglement mediated by the glycol chains on the **OTgCS** macrocycles and/or the dissociation of the 2:2 supramolecular linkages upon heating. The adhesion strength could be recovered by overlapping the two slides together and storing them under vacuum for 1 hour. Presumably, the supramolecular polymer is able to dynamically reform at the physically contacted interface. This reversible process could be repeated for a few cycles without losing the base adhesion strength.

On account of the dynamic and stimuli-responsive characteristics of supramolecular linkages, the reusability<sup>91-93</sup> we showed here or interfacial self-healing properties<sup>14,94-95</sup> are typical features of supramolecular polymer adhesives. However, to the best of our knowledge, this is the first report that demonstrates a supramolecular polymer with tunable adhesion strength based on controlling the polymer sequence (Figure 8c). Specifically, the homopolymer (**A**)<sub>n</sub> shows comparable adhesion strength to commercial superglue formulations based on polycyanoacrylate (5~9 MPa, Table 1),<sup>73</sup> while the adhesion strength of the copolymer (**AB**)<sub>n</sub> is comparable to white glue based on poly(vinyl acetate) (0.43 MPa, Table 1).<sup>74</sup> Thus, we can tune the adhesion strength of the supramolecular polymer between that of superglue and white glue simply by changing the stoichiometric ratio of the monomers (Figure 8c). Consistently, we also see an intermediate mixture of cyanostar with 0.75 equivalent of phenylene diphosphate shows a  $2.1 \pm 0.3$  MPa pull-off strength and  $0.9 \pm 0.2$  MPa lap-shear strength. The properties stem directly from the sequence-

1  
2  
3 defined structures and the strengths of the supramolecular linkage chemistries. This study provides  
4  
5 a new way to understand how material properties reflect structural information in the form of  
6  
7 anion-driven supramolecular polymer adhesives.  
8  
9

## 10 11 12 13 **Conclusions**

14  
15  
16 We discovered a new form of sequence control in supramolecular polymers based on  
17  
18 diphosphate monomers of compact size mixed with cyanostar macrocycles to drive phosphate-  
19  
20 phosphate dimerization. With a 2:1 stoichiometry, a supramolecular homopolymer (**A**)<sub>n</sub> is  
21  
22 produced that is composed of phosphate-phosphate dimers inside  $\pi$ -stacked cyanostar macrocycles.  
23  
24 At a 1:1 stoichiometry, the alternating supramolecular copolymer (**AB**)<sub>n</sub> is co-driven by cyanostar-  
25  
26 stabilized phosphate dimers and cation-stabilized phosphate dimers. The cation-stabilized dimers  
27  
28 emerge hierarchically from the superstructure in which the stronger primary cyanostar-stabilized  
29  
30 linkages liberate extra cations that are used to reinforce the secondary ionic linkage. The two types  
31  
32 of anion-anion dimers constitute orthogonal linkage chemistries, which are required to elicit  
33  
34 sequence control. This study further demonstrates the utility of anion-anion dimerization to  
35  
36 synthesize functional and tunable supramolecular polymers. This is the first time that these  
37  
38 linkages have been transformed into a polymer capable of supporting materials properties  
39  
40 expressed here as adhesion. The supramolecular homopolymer (**A**)<sub>n</sub> displays strong adhesive  
41  
42 properties, whereas the alternating supramolecular copolymer (**AB**)<sub>n</sub> has less adhesion strength.  
43  
44 Here we see expression of the remarkable idea that sum of attractive driving forces in the anion-  
45  
46 anion linkages overcome their repulsions when stabilized by complementary cyanostar receptors  
47  
48 to a greater extent than traditional ionic contacts. Thus, the adhesion strength of the supramolecular  
49  
50 polymers is composition-dependent, which corresponds directly to the stoichiometry- and  
51  
52  
53  
54  
55  
56  
57

1  
2  
3 sequenced-controlled state of polymerization. We believe that this study lays a foundation for a  
4  
5 broad variety of anion-based materials with customized properties derived from custom-designed  
6  
7 anions and helps to expand the scope of anion-relevant supramolecular systems.  
8  
9

## 10 11 **ASSOCIATED CONTENT**

### 12 13 **Supporting Information**

14  
15 The Supporting Information is available free of charge on the ACS Publication website.

16  
17 General methods, synthetic procedures, crystallography,  $^1\text{H}$  NMR titrations, 2D NMR analysis,  
18  
19 diffusion NMR studies, viscosity measurement, weight-lifting test,  $^1\text{H}$  and  $^{13}\text{C}$  NMR  
20  
21 characterizations.  
22  
23  
24  
25

## 26 27 **AUTHOR INFORMATION**

### 28 29 **Corresponding Authors**

30  
31 [\\*aflood@indiana.edu](mailto:*aflood@indiana.edu)

### 32 33 **Present Addresses**

34  
35 §B.Q.: Research Laboratory of Electronics, Massachusetts Institute of Technology, Cambridge,  
36  
37 MA 02139  
38

### 39 40 **Notes**

41  
42 The authors declare no competing financial interests.  
43  
44

## 45 46 **ACKNOWLEDGEMENTS**

47  
48 AHF acknowledges support from the National Science Foundation (CHE 1709909). JDA  
49  
50 acknowledges support from the National Science Foundation (OIA 1632825). JT acknowledges  
51  
52 traineeship support from the NSF NRT program “Interface” (DGE 1449999) through the  
53  
54 University of Southern Mississippi.  
55  
56  
57

## REFERENCES

- (1) Yanagisawa, Y.; Nan, Y.; Okuro, K.; Aida, T. Mechanically robust, readily repairable polymers via tailored noncovalent cross-linking. *Science* **2018**, *359*, 72.
- (2) Gu, Y.; Alt, E. A.; Wang, H.; Li, X.; Willard, A. P.; Johnson, J. A. Photoswitching topology in polymer networks with metal–organic cages as crosslinks. *Nature* **2018**, *560*, 65.
- (3) Brunsveld, L.; Folmer, B.; Meijer, E. W.; Sijbesma, R. Supramolecular polymers. *Chem. Rev.* **2001**, *101*, 4071.
- (4) Dankers, P. Y.; Harmsen, M. C.; Brouwer, L. A.; Van Luyn, M. J.; Meijer, E. A modular and supramolecular approach to bioactive scaffolds for tissue engineering. *Nat. Mater.* **2005**, *4*, 568.
- (5) Aida, T.; Meijer, E.; Stupp, S. Functional supramolecular polymers. *Science* **2012**, *335*, 813.
- (6) Lutz, J.-F.; Lehn, J.-M.; Meijer, E.; Matyjaszewski, K. From precision polymers to complex materials and systems. *Nat. Rev. Mater.* **2016**, *1*, 16024.
- (7) Vantomme, G.; Meijer, E. The construction of supramolecular systems. *Science* **2019**, *363*, 1396.
- (8) Lehn, J. M. Perspectives in supramolecular chemistry—from molecular recognition towards molecular information processing and self-organization. *Angew. Chem. Int. Ed. Eng.* **1990**, *29*, 1304.
- (9) Lehn, J.-M. From supramolecular chemistry towards constitutional dynamic chemistry and adaptive chemistry. *Chem. Soc. Rev.* **2007**, *36*, 151.
- (10) Webber, M. J.; Appel, E. A.; Meijer, E.; Langer, R. Supramolecular biomaterials. *Nat. Mater.* **2016**, *15*, 13.

- 1  
2  
3 (11) Zou, L.; Braegelman, A. S.; Webber, M. J. Spatially Defined Drug Targeting by in Situ  
4 Host–Guest Chemistry in a Living Animal. *ACS Cent. Sci.* **2019**, *5*, 1035.  
5  
6  
7 (12) Li, C.-H.; Wang, C.; Keplinger, C.; Zuo, J.-L.; Jin, L.; Sun, Y.; Zheng, P.; Cao, Y.; Lissel,  
8 F.; Linder, C.; You, X.-Z.; Bao, Z. A highly stretchable autonomous self-healing elastomer.  
9 *Nat. Chem.* **2016**, *8*, 618.  
10  
11  
12 (13) Choi, S.; Kwon, T.-w.; Coskun, A.; Choi, J. W. Highly elastic binders integrating  
13 polyrotaxanes for silicon microparticle anodes in lithium ion batteries. *Science* **2017**, *357*,  
14 279.  
15  
16  
17 (14) Ji, X.; Wu, R. T.; Long, L.; Ke, X. S.; Guo, C.; Ghang, Y. J.; Lynch, V. M.; Huang, F.;  
18 Sessler, J. L. Encoding, Reading, and Transforming Information Using Multifluorescent  
19 Supramolecular Polymeric Hydrogels. *Adv. Mater.* **2018**, *30*, 1705480.  
20  
21  
22 (15) Burnworth, M.; Tang, L.; Kumpfer, J. R.; Duncan, A. J.; Beyer, F. L.; Fiore, G. L.; Rowan,  
23 S. J.; Weder, C. Optically healable supramolecular polymers. *Nature* **2011**, *472*, 334.  
24  
25  
26 (16) Lutz, J.-F.; Ouchi, M.; Liu, D. R.; Sawamoto, M. Sequence-controlled polymers. *Science*  
27 **2013**, *341*, 1238149.  
28  
29  
30 (17) Wei, P.; Yan, X.; Cook, T. R.; Ji, X.; Stang, P. J.; Huang, F. Supramolecular Copolymer  
31 Constructed by Hierarchical Self-Assembly of Orthogonal Host-Guest, H-Bonding, and  
32 Coordination Interactions. *ACS Macro Lett.* **2016**, *5*, 671.  
33  
34  
35 (18) Wei, P.; Yan, X.; Huang, F. Supramolecular polymers constructed by orthogonal self-  
36 assembly based on host–guest and metal–ligand interactions. *Chem. Soc. Rev.* **2015**, *44*,  
37 815.  
38  
39  
40  
41  
42  
43  
44  
45  
46  
47  
48  
49  
50  
51  
52  
53  
54  
55  
56  
57  
58  
59  
60

- 1  
2  
3 (19) Yan, X.; Cook, T. R.; Pollock, J. B.; Wei, P.; Zhang, Y.; Yu, Y.; Huang, F.; Stang, P. J.  
4  
5 Responsive supramolecular polymer metallogel constructed by orthogonal coordination-  
6  
7 driven self-assembly and host/guest interactions. *J. Am. Chem. Soc.* **2014**, *136*, 4460.  
8  
9  
10 (20) Wang, F.; Han, C.; He, C.; Zhou, Q.; Zhang, J.; Wang, C.; Li, N.; Huang, F. Self-sorting  
11  
12 organization of two heteroditopic monomers to supramolecular alternating copolymers. *J.*  
13  
14 *Am. Chem. Soc.* **2008**, *130*, 11254.  
15  
16  
17 (21) Kim, D. S.; Chang, J.; Leem, S.; Park, J. S.; Thordarson, P.; Sessler, J. L. Redox-and pH-  
18  
19 Responsive Orthogonal Supramolecular Self-Assembly: An Ensemble Displaying  
20  
21 Molecular Switching Characteristics. *J. Am. Chem. Soc.* **2015**, *137*, 16038.  
22  
23  
24 (22) Zeng, F.; Han, Y.; Chen, C.-F. Self-sorting behavior of a four-component host–guest  
25  
26 system and its incorporation into a linear supramolecular alternating copolymer. *Chem.*  
27  
28 *Commun.* **2015**, *51*, 3593.  
29  
30  
31 (23) Besenius, P. Controlling supramolecular polymerization through multicomponent self-  
32  
33 assembly. *J. Polym. Sci. Part A: Polym. Chem.* **2017**, *55*, 34.  
34  
35  
36 (24) Li, H.; Fan, X.; Min, X.; Qian, Y.; Tian, W. Controlled Supramolecular Architecture  
37  
38 Transformation from Homopolymer to Copolymer through Competitive Self-Sorting  
39  
40 Method. *Macromol. Rapid Commun.* **2017**, *38*, 1600631.  
41  
42  
43 (25) Chakraborty, S.; Ray, D.; Aswal, V. K.; Ghosh, S. Multi-Stimuli-Responsive Directional  
44  
45 Assembly of an Amphiphilic Donor–Acceptor Alternating Supramolecular Copolymer.  
46  
47 *Chem. Eur. J.* **2018**, *24*, 16379.  
48  
49  
50 (26) Nadamoto, K.; Maruyama, K.; Fujii, N.; Ikeda, T.; Kihara, S. i.; Haino, T. Supramolecular  
51  
52 Copolymerization by Sequence Reorganization of a Supramolecular Homopolymer.  
53  
54 *Angew. Chem. Int. Ed.* **2018**, *57*, 7028.  
55  
56  
57  
58  
59  
60

- 1  
2  
3 (27) Hirao, T.; Kudo, H.; Amimoto, T.; Haino, T. Sequence-controlled supramolecular  
4 terpolymerization directed by specific molecular recognitions. *Nat. Commun.* **2017**, *8*, 634.  
5  
6  
7 (28) Raeisi, M.; Kotturi, K.; del Valle, I.; Schulz, J.; Dornblut, P.; Masson, E. Sequence-Specific  
8 Self-Assembly of Positive and Negative Monomers with Cucurbit[8]uril Linkers. *J. Am.*  
9 *Chem. Soc.* **2018**, *140*, 3371.  
10  
11  
12 (29) Xiujuan, S.; Zhang, X.; Ni, X.-L.; Zhang, H.; Wei, P.; Liu, J.; Xing, H.; Peng, H.-Q.; Lam,  
13 J. W.; Zhang, P. Supramolecular Polymerization with Dynamic Self-Sorting Sequence  
14 Control. *Macromolecules* **2019**, *52*, 8814.  
15  
16  
17 (30) Wang, X.; Han, K.; Li, J.; Jia, X.; Li, C. Pillar[5]arene–neutral guest recognition based  
18 supramolecular alternating copolymer containing [c2] daisy chain and bis-pillar[5]arene  
19 units. *Polym. Chem.* **2013**, *4*, 3998.  
20  
21  
22 (31) Felder, T.; de Greef, T. F.; Nieuwenhuizen, M. M.; Sijbesma, R. P. Alternation and tunable  
23 composition in hydrogen bonded supramolecular copolymers. *Chem. Commun.* **2014**, *50*,  
24 2455.  
25  
26  
27 (32) Ahmed, S.; Singha, N.; Pramanik, B.; Mondal, J. H.; Das, D. Redox controlled reversible  
28 transformation of a supramolecular alternating copolymer to a radical cation containing  
29 homo-polymer. *Polym. Chem.* **2016**, *7*, 4393.  
30  
31  
32 (33) Chakraborty, S.; Kar, H.; Sikder, A.; Ghosh, S. Steric ploy for alternating donor–acceptor  
33 co-assembly and cooperative supramolecular polymerization. *Chem. Sci.* **2017**, *8*, 1040.  
34  
35  
36 (34) He, Z.; Jiang, W.; Schalley, C. A. Integrative self-sorting: a versatile strategy for the  
37 construction of complex supramolecular architecture. *Chem. Soc. Rev.* **2015**, *44*, 779.  
38  
39  
40  
41  
42  
43  
44  
45  
46  
47  
48  
49  
50  
51  
52  
53  
54  
55  
56  
57  
58  
59  
60

- 1  
2  
3 (35) Adelizzi, B.; Van Zee, N. J.; de Windt, L. N.; Palmans, A. R.; Meijer, E. W. Future of  
4  
5 supramolecular copolymers unveiled by reflecting on covalent copolymerization. *J. Am.*  
6  
7 *Chem. Soc.* **2019**, *141*, 6110.  
8  
9  
10 (36) Complementary names for the homopolymer and alternating copolymer are poly(pseudo  
11  
12 rotaxane) and poly(pseudo rotaxane) with a periodically defined location of the ring parts,  
13  
14 respectively.  
15  
16  
17 (37) Lee, J.; Ghosh, K.; Stang, P. J. Stoichiometric control of multiple different tectons in  
18  
19 coordination-driven self-assembly: preparation of fused metallacyclic polygons. *J. Am.*  
20  
21 *Chem. Soc.* **2009**, *131*, 12028.  
22  
23  
24 (38) D'Urso, A.; Cristaldi, D. A.; Fragalà, M. E.; Gattuso, G.; Pappalardo, A.; Villari, V.; Micali,  
25  
26 N.; Pappalardo, S.; Parisi, M. F.; Purrello, R. Sequence, Stoichiometry, and Dimensionality  
27  
28 Control in Porphyrin/Bis-calix[4]arene Self-Assemblies in Aqueous Solution. *Chem. Eur.*  
29  
30 *J.* **2010**, *16*, 10439.  
31  
32  
33 (39) Lin, C.; Xu, L.; Huang, L.; Chen, J.; Liu, Y.; Ma, Y.; Ye, F.; Qiu, H.; Tian, H.; Yin, S.  
34  
35 Metal Coordination Stoichiometry Controlled Formation of Linear and Hyperbranched  
36  
37 Supramolecular Polymers. *Macromol. Rapid Commun.* **2016**, *37*, 1453.  
38  
39  
40 (40) Wang, F.; Feng, C. L. Stoichiometry-Controlled Inversion of Supramolecular Chirality in  
41  
42 Nanostructures Co-assembled with Bipyridines. *Chem. Eur. J.* **2018**, *24*, 1509.  
43  
44  
45 (41) Ji, W.; Yuan, C.; Chakraborty, P.; Gilead, S.; Yan, X.; Gazit, E. Stoichiometry-controlled  
46  
47 secondary structure transition of amyloid-derived supramolecular dipeptide co-assemblies.  
48  
49 *Commun. Chem.* **2019**, *2*, 65.  
50  
51  
52  
53  
54  
55  
56  
57  
58  
59  
60

- 1  
2  
3 (42) Li, P.; Lü, B.; Han, D.; Duan, P.; Liu, M.; Yin, M. Stoichiometry-controlled inversion of  
4 circularly polarized luminescence in co-assembly of chiral gelators with an achiral  
5 tetraphenylethylene derivative. *Chem. Commun.* **2019**, *55*, 2194.  
6  
7  
8  
9  
10 (43) Gong, H.-Y.; Rambo, B. M.; Karnas, E.; Lynch, V. M.; Sessler, J. L. A ‘Texas-  
11 sized’ molecular box that forms an anion-induced supramolecular necklace. *Nat. Chem.*  
12 **2010**, *2*, 406.  
13  
14  
15  
16 (44) Whittell, G. R.; Hager, M. D.; Schubert, U. S.; Manners, I. Functional soft materials from  
17 metallopolymers and metallosupramolecular polymers. *Nat. Mater.* **2011**, *10*, 176.  
18  
19  
20 (45) Scherman, O. A.; Ligthart, G.; Sijbesma, R. P.; Meijer, E. A Selectivity-Driven  
21 Supramolecular Polymerization of an AB Monomer. *Angew. Chem. Int. Ed.* **2006**, *45*, 2072.  
22  
23  
24  
25 (46) Qin, B.; Zhang, S.; Song, Q.; Huang, Z.; Xu, J. F.; Zhang, X. Supramolecular Interfacial  
26 Polymerization: A Controllable Method of Fabricating Supramolecular Polymeric  
27 Materials. *Angew. Chem. Int. Ed.* **2017**, *56*, 7639.  
28  
29  
30  
31 (47) Ogi, S.; Sugiyasu, K.; Manna, S.; Samitsu, S.; Takeuchi, M. Living supramolecular  
32 polymerization realized through a biomimetic approach. *Nat. Chem.* **2014**, *6*, 188.  
33  
34  
35  
36 (48) Weingarten, A. S.; Kazantsev, R. V.; Palmer, L. C.; McClendon, M.; Koltonow, A. R.;  
37 Samuel, A. P.; Kiebal, D. J.; Wasielewski, M. R.; Stupp, S. I. Self-assembling hydrogel  
38 scaffolds for photocatalytic hydrogen production. *Nat. Chem.* **2014**, *6*, 964.  
39  
40  
41  
42 (49) Dong, S.; Luo, Y.; Yan, X.; Zheng, B.; Ding, X.; Yu, Y.; Ma, Z.; Zhao, Q.; Huang, F. A  
43 dual-responsive supramolecular polymer gel formed by crown ether based molecular  
44 recognition. *Angew. Chem. Int. Ed.* **2011**, *50*, 1905.  
45  
46  
47  
48 (50) Chen, H.; Huang, Z.; Wu, H.; Xu, J. F.; Zhang, X. Supramolecular Polymerization  
49 Controlled through Kinetic Trapping. *Angew. Chem. Int. Ed.* **2017**, *56*, 16575.  
50  
51  
52  
53  
54  
55  
56  
57  
58  
59  
60

- 1  
2  
3 (51) McDonald, K. P.; Qiao, B.; Twum, E. B.; Lee, S.; Gamache, P. J.; Chen, C.-H.; Yi, Y.;  
4  
5 Flood, A. H. Quantifying chloride binding and salt extraction with poly(methyl  
6  
7 methacrylate) copolymers bearing aryl-triazoles as anion receptor side chains. *Chem.*  
8  
9 *Commun.* **2014**, *50*, 13285.
- 10  
11  
12 (52) Zhao, W.; Qiao, B.; Tropp, J.; Pink, M.; Azoulay, J. D.; Flood, A. H. Linear  
13  
14 Supramolecular Polymers Driven by Anion–Anion Dimerization of Difunctional  
15  
16 Phosphonate Monomers Inside Cyanostar Macrocycles. *J. Am. Chem. Soc.* **2019**, *141*, 4980.
- 17  
18  
19 (53) Capici, C.; Cohen, Y.; D'Urso, A.; Gattuso, G.; Notti, A.; Pappalardo, A.; Pappalardo, S.;  
20  
21 Parisi, M. F.; Purrello, R.; Slovak, S. Anion-Assisted Supramolecular Polymerization:  
22  
23 From Achiral AB-Type Monomers to Chiral Assemblies. *Angew. Chem. Int. Ed.* **2011**, *50*,  
24  
25 11956.
- 26  
27  
28 (54) Rostami, A.; Wei, C. J.; Guérin, G.; Taylor, M. S. Anion Detection by a Fluorescent Poly  
29  
30 (squaramide): Self-Assembly of Anion-Binding Sites by Polymer Aggregation. *Angew.*  
31  
32 *Chem. Int. Ed.* **2011**, *50*, 2059.
- 33  
34  
35 (55) Gong, H.-Y.; Rambo, B. M.; Lynch, V. M.; Keller, K. M.; Sessler, J. L. “Texas-Sized”  
36  
37 Molecular Boxes: Building Blocks for the Construction of Anion-Induced Supramolecular  
38  
39 Species via Self-Assembly. *J. Am. Chem. Soc.* **2013**, *135*, 6330.
- 40  
41  
42 (56) Silver, E. S.; Rambo, B. M.; Bielawski, C. W.; Sessler, J. L. Reversible Anion-Induced  
43  
44 Cross-Linking of Well-Defined Calix[4]pyrrole-Containing Copolymers. *J. Am. Chem.*  
45  
46 *Soc.* **2014**, *136*, 2252.
- 47  
48  
49 (57) Zhang, Z.; Kim, D. S.; Lin, C.-Y.; Zhang, H.; Lammer, A. D.; Lynch, V. M.; Popov, I.;  
50  
51 Miljanić, O. S.; Anslyn, E. V.; Sessler, J. L. Expanded porphyrin-anion supramolecular  
52  
53  
54  
55  
56  
57  
58  
59  
60

- 1  
2  
3 assemblies: environmentally responsive sensors for organic solvents and anions. *J. Am.*  
4  
5 *Chem. Soc.* **2015**, *137*, 7769.  
6  
7  
8 (58) Tepper, R.; Bode, S.; Geitner, R.; Jäger, M.; Görls, H.; Vitz, J.; Dietzek, B.; Schmitt, M.;  
9  
10 Popp, J.; Hager, M. D. Polymeric Halogen-Bond-Based Donor Systems Showing Self-  
11  
12 Healing Behavior in Thin Films. *Angew. Chem. Int. Ed.* **2017**, *56*, 4047.  
13  
14 (59) Zapata, F.; González, L.; Caballero, A.; Bastida, A.; Bautista, D.; Molina, P. Interlocked  
15  
16 Supramolecular Polymers Created by Combination of Halogen- and Hydrogen-Bonding  
17  
18 Interactions through Anion-Template Self-Assembly. *J. Am. Chem. Soc.* **2018**, *140*, 2041.  
19  
20 (60) Weinhold, F.; Klein, R. A. Anti-Electrostatic Hydrogen Bonds. *Angew. Chem. Int. Ed.*  
21  
22 **2014**, *53*, 11214.  
23  
24  
25 (61) Frenking, G.; Caramori, G. F. No Need for a Re-examination of the Electrostatic Notation  
26  
27 of the Hydrogen Bonding: A Comment. *Angew. Chem. Int. Ed.* **2015**, *54*, 2596.  
28  
29  
30 (62) Mata, I.; Molins, E.; Alkorta, I.; Espinosa, E. The Paradox of Hydrogen-Bonded Anion–  
31  
32 Anion Aggregates in Oxoanions: A Fundamental Electrostatic Problem Explained in  
33  
34 Terms of Electrophilic···Nucleophilic Interactions. *J. Phys. Chem. A* **2015**, *119*, 183.  
35  
36 (63) Weinhold, F.; Klein, R. A. Improved General Understanding of the Hydrogen-Bonding  
37  
38 Phenomena: A Reply. *Angew. Chem. Int. Ed.* **2015**, *54*, 2600.  
39  
40  
41 (64) Knorr, A.; Stange, P.; Fumino, K.; Weinhold, F.; Ludwig, R. Spectroscopic Evidence for  
42  
43 Clusters of Like-Charged Ions in Ionic Liquids Stabilized by Cooperative Hydrogen  
44  
45 Bonding. *ChemPhysChem* **2016**, *17*, 458.  
46  
47  
48 (65) Cullen, D. A.; Gardiner, M. G.; White, N. G. A three dimensional hydrogen bonded organic  
49  
50 framework assembled through antielectrostatic hydrogen bonds. *Chem. Commun.* **2019**, *55*,  
51  
52 12020.  
53  
54  
55  
56  
57  
58  
59  
60

- 1  
2  
3 (66) White, N. G. Antielectrostatically hydrogen bonded anion dimers: counter-intuitive,  
4 common and consistent. *CrystEngComm* **2019**, *21*, 4855.  
5  
6  
7 (67) Fatila, E. M.; Twum, E. B.; Sengupta, A.; Pink, M.; Karty, J. A.; Raghavachari, K.; Flood,  
8 A. H. Anions Stabilize Each Other inside Macrocyclic Hosts. *Angew. Chem. Int. Ed.* **2016**,  
9 *55*, 14057.  
10  
11  
12 (68) Fatila, E. M.; Twum, E. B.; Karty, J. A.; Flood, A. H. Ion-pairing and Co-facial Stacking  
13 Drive High-fidelity Bisulfate Assembly with Cyanostar Macrocyclic Hosts. *Chem. Eur. J.*  
14 **2017**, *23*, 10652.  
15  
16  
17 (69) Dobscha, J. R.; Debnath, S.; Fadler, R. E.; Fatila, E. M.; Pink, M.; Raghavachari, K.; Flood,  
18 A. H. Host-host Interactions Control Self-assembly and Switching of Triple and Double  
19 Decker Stacks of Tricarbazole Macrocycles Co-assembled with *Anti*-electrostatic Bisulfate  
20 Dimers. *Chem. Eur. J.* **2018**, *24*, 9841.  
21  
22  
23 (70) Zhao, W.; Qiao, B.; Chen, C. H.; Flood, A. H. High-Fidelity Multistate Switching with  
24 Anion–Anion and Acid–Anion Dimers of Organophosphates in Cyanostar Complexes.  
25 *Angew. Chem. Int. Ed.* **2017**, *56*, 13083.  
26  
27  
28 (71) Fatila, E. M.; Pink, M.; Twum, E. B.; Karty, J. A.; Flood, A. H. Phosphate-phosphate  
29 oligomerization drives higher order co-assemblies with stacks of cyanostar macrocycles.  
30 *Chem. Sci.* **2018**, *9*, 2863.  
31  
32  
33 (72) Lee, S.; Chen, C.-H.; Flood, A. H. A pentagonal cyanostar macrocycle with cyanostilbene  
34 CH donors binds anions and forms dialkylphosphate [3]rotaxanes. *Nat. Chem.* **2013**, *5*, 704.  
35  
36  
37 (73) Heinzmann, C.; Weder, C.; de Espinosa, L. M. Supramolecular polymer adhesives:  
38 advanced materials inspired by nature. *Chem. Soc. Rev.* **2016**, *45*, 342.  
39  
40  
41  
42  
43  
44  
45  
46  
47  
48  
49  
50  
51  
52  
53  
54  
55  
56  
57  
58  
59  
60

- 1  
2  
3 (74) Dong, S.; Leng, J.; Feng, Y.; Liu, M.; Stackhouse, C. J.; Schönhals, A.; Chiappisi, L.; Gao,  
4 L.; Chen, W.; Shang, J. Structural water as an essential comonomer in supramolecular  
5 polymerization. *Sci. Adv.* **2017**, *3*, eaao0900.  
6  
7  
8  
9  
10 (75) Gebbie, M. A.; Wei, W.; Schrader, A. M.; Cristiani, T. R.; Dobbs, H. A.; Idso, M.; Chmelka,  
11 B. F.; Waite, J. H.; Israelachvili, J. N. Tuning underwater adhesion with cation- $\pi$   
12 interactions. *Nat. Chem.* **2017**, *9*, 473.  
13  
14  
15  
16  
17 (76) Li, J.; Celiz, A.; Yang, J.; Yang, Q.; Wamala, I.; Whyte, W.; Seo, B.; Vasilyev, N.; Vlassak,  
18 J.; Suo, Z. Tough adhesives for diverse wet surfaces. *Science* **2017**, *357*, 378.  
19  
20  
21 (77) Liu, J.; Tan, C. S. Y.; Scherman, O. A. Dynamic Interfacial Adhesion through  
22 Cucurbit[n]uril Molecular Recognition. *Angew. Chem. Int. Ed.* **2018**, *130*, 8992.  
23  
24  
25  
26 (78) Zhang, Q.; Shi, C.-Y.; Qu, D.-H.; Long, Y.-T.; Feringa, B. L.; Tian, H. Exploring a  
27 naturally tailored small molecule for stretchable, self-healing, and adhesive supramolecular  
28 polymers. *Sci. Adv.* **2018**, *4*, eaat8192.  
29  
30  
31  
32  
33 (79) Saiz-Poseu, J.; Mancebo-Aracil, J.; Nador, F.; Busqué, F.; Ruiz-Molina, D. The Chemistry  
34 behind Catechol-Based Adhesion. *Angew. Chem. Int. Ed.* **2019**, *58*, 696.  
35  
36  
37 (80) Zhang, Q.; Li, T.; Duan, A.; Dong, S.; Zhao, W.; Stang, P. J. Formation of a  
38 Supramolecular Polymeric Adhesive via Water-Participant Hydrogen Bonding Formation.  
39 *J. Am. Chem. Soc.* **2019**, *141*, 8058.  
40  
41  
42  
43  
44 (81) Liu, Y.; Singharoy, A.; Mayne, C. G.; Sengupta, A.; Raghavachari, K.; Schulten, K.; Flood,  
45 A. H. Flexibility Coexists with Shape-Persistence in Cyanostar Macrocycles. *J. Am. Chem.*  
46 *Soc.* **2016**, *138*, 4843.  
47  
48  
49  
50  
51  
52  
53  
54  
55  
56  
57  
58  
59  
60

- 1  
2  
3 (82) Sheetz, E. G.; Qiao, B.; Pink, M.; Flood, A. H. Programmed Negative Allostery with  
4 Guest-Selected Rotamers Control Anion–Anion Complexes of Stackable Macrocycles. *J.*  
5 *Am. Chem. Soc.* **2018**, *140*, 7773.  
6  
7  
8  
9  
10 (83) Gerasimchuk, O. A.; Mason, S.; Llinares, J. M.; Song, M.; Alcock, N. W.; Bowman-James,  
11 K. Binding of phosphate with a simple hexaaza polyammonium macrocycle. *Inorg. Chem.*  
12 **2000**, *39*, 1371.  
13  
14  
15  
16  
17 (84) Němec, I.; Macháčková, Z.; Teubner, K.; Císařová, I.; Vaněk, P.; Mička, Z. The structural  
18 phase transitions of aminoguanidinium (1<sup>+</sup>) dihydrogen phosphate–study of crystal  
19 structures, vibrational spectra and thermal behavior. *J. Solid State Chem.* **2004**, *177*, 4655.  
20  
21  
22  
23  
24 (85) Dhara, A.; Flood, A. H. Cages Driven Away from Equilibrium Binding by Electric Fields.  
25 *Chem* **2019**, *5*, 1017.  
26  
27  
28  
29 (86) Borsley, S.; Haugland, M. M.; Oldknow, S.; Cooper, J. A.; Burke, M. J.; Scott, A.;  
30 Grantham, W.; Vallejo, J.; Brechin, E. K.; Lusby, P. J. Electrostatic forces in field-  
31 perturbed equilibria: nanopore analysis of cage complexes. *Chem* **2019**, *5*, 1275.  
32  
33  
34  
35 (87) Zhang, J.; Pesak, D. J.; Ludwick, J. L.; Moore, J. S. Geometrically-controlled and site-  
36 specifically-functionalized phenylacetylene macrocycles. *J. Am. Chem. Soc.* **1994**, *116*,  
37 4227.  
38  
39  
40  
41  
42 (88) Li, Y.; Flood, A. H. Strong, Size-Selective, and Electronically Tunable C–H···Halide  
43 Binding with Steric Control over Aggregation from Synthetically Modular, Shape-  
44 Persistent [3<sub>4</sub>]Triazolophanes. *J. Am. Chem. Soc.* **2008**, *130*, 12111.  
45  
46  
47  
48  
49 (89) Niu, Z.; Huang, F.; Gibson, H. W. Supramolecular AA–BB-type linear polymers with  
50 relatively high molecular weights via the self-assembly of bis (m-phenylene)-32-crown-10  
51 cryptands and a bisparaquat derivative. *J. Am. Chem. Soc.* **2011**, *133*, 2836.  
52  
53  
54  
55  
56  
57  
58  
59  
60

- 1  
2  
3 (90) Yang, L.; Tan, X.; Wang, Z.; Zhang, X. Supramolecular polymers: historical development,  
4 preparation, characterization, and functions. *Chem. Rev.* **2015**, *115*, 7196.  
5  
6  
7 (91) Heinzmann, C.; Coulibaly, S.; Roulin, A.; Fiore, G. L.; Weder, C. Light-induced bonding  
8 and debonding with supramolecular adhesives. *ACS Appl. Mater. Interfaces* **2014**, *6*, 4713.  
9  
10  
11 (92) Michal, B. T.; Spencer, E. J.; Rowan, S. J. Stimuli-responsive reversible two-level adhesion  
12 from a structurally dynamic shape-memory polymer. *ACS Appl. Mater. Interfaces* **2016**, *8*,  
13 11041.  
14  
15  
16  
17 (93) Liu, J.; Scherman, O. A. Cucurbit[n]uril Supramolecular Hydrogel Networks as Tough and  
18 Healable Adhesives. *Adv. Funct. Mater.* **2018**, *28*, 1800848.  
19  
20  
21  
22 (94) Harada, A.; Kobayashi, R.; Takashima, Y.; Hashidzume, A.; Yamaguchi, H. Macroscopic  
23 self-assembly through molecular recognition. *Nat. Chem.* **2011**, *3*, 34.  
24  
25  
26  
27 (95) Liu, J.; Tan, C. S. Y.; Yu, Z.; Li, N.; Abell, C.; Scherman, O. A. Tough Supramolecular  
28 Polymer Networks with Extreme Stretchability and Fast Room-Temperature Self-Healing.  
29 *Adv. Mater.* **2017**, *29*, 1605325.  
30  
31  
32  
33  
34  
35  
36  
37  
38  
39  
40  
41  
42  
43  
44  
45  
46  
47  
48  
49  
50  
51  
52  
53  
54  
55  
56  
57  
58  
59  
60

For Table of Contents Only

